



VYSOKÉ UČENÍ TECHNICKÉ V BRNĚ
BRNO UNIVERSITY OF TECHNOLOGY



FAKULTA CHEMICKÁ
ÚSTAV FYZIKÁLNÍ A SPOTŘEBNÍ CHEMIE

FACULTY OF CHEMISTRY
INSTITUTE OF PHYSICAL AND APPLIED CHEMISTRY

MODELLING OF CHEMICAL PROCESSES

MODELOVÁNÍ CHEMICKÝCH PROCESŮ

DIZERTAČNÍ PRÁCE

DOCTORAL THESIS

AUTOR PRÁCE
AUTHOR

Mgr. AMER AL MAHMOUD ALSHEIKH

VEDOUCÍ PRÁCE
SUPERVISOR

Mgr. JAN ŽÍDEK, Ph.D.

BRNO 2015

ABSTRACT

In this thesis the study of the fragmentation process of certain molecule is presented and it has been used to know the nature of fragmentation products. This work is concentrated to the calculation of fragmentation energy of the molecule using *ab initio* quantum chemistry methods and density functional theory (DFT) calculations and with a support by experiment. The influence of the computational method, basis set, and the geometry of molecule on simulation has been presented.

It was compared the fragmentaion of methylphenylsilane (MPS), dimethylphenylsilane (DMPS) and trimethylphenylsilane (TMPS). The fragmentation was initiated by electron impact ionization (EII). The mass spectrometry technique was used to the analysis of the composition of fragmentation products from MPS and TMPS. The fragmentation products measured in this work were interpreted with respect to the ionization energy, appearance energies of fragments and bond dissociation energy of selected bonds. The results for MPS and TMPS were completed with DMPS previously published experimental data in order to have the series of similar compounds, which differ only by number of CH₃ groups. Even the structurally similar molecules have significantly different fragmentation behavior. Comparison with the theoretical bond dissociation energies calculated using the DFT calculations has been presented.

Using the combined experimental and theoretical approaches we have focused our recent studies to the common features as well as basic differences of the fragmentation schemes of all the three molecules. We proposed subtraction of two hydrogen atoms during plasma induced fragmentation process. The subtraction of H₂ molecule, specific for MPS but rarely observed also in the other two compounds was also of high interest in our studies. It can run in two mechanisms: i. subtraction of two hydrogens one-by-one and ii. dissociation of H₂ in one step. We can predict which mechanism is more probable according to the DFT calculated energy profile of reaction. The calculated predictions were in correlation with the composition of fragmentation products from experimental mass spectra.

ABSTRAKT

V této práci je prezentována studie fragmentačního procesu zvolené molekuly a jeho vztah ke složení fragmentačních produktů. Práce je zaměřená na výpočet fragmentační energie molekuly pomocí *ab initio* kvantově chemických metod, metodou „density functional theory (DFT)“ a také srovnáním s experimentem. Je prezentován vliv výpočetní metody, bázeového setu, a geometrie molekuly na simulaci.

Byla porovnána fragmentace methylfenylsilanu (MPS), dimethylfenylsilanu (DMPS), a trimethylfenylsilanu (TMPS). Fragmentace byla iniciována monochromatickým elektronovým svazkem (EII). Hmotnostní spektrometrie byla využita ke studiu složení fragmentačních produktů MPS a TMPS. Fragmentační produkty MPS a TMPS měřené v rámci této práce byly doplněny o experimentální studii DMPS, která byla prezentována v literatuře. Takto byla získána řada molekul, které jsou strukturně podobné, ale mají výrazně rozdílné chování během fragmentace. Pomocí měření účinného průřezu byly měřeny disociační energie vazeb a tyto disociační energie byly vypočteny pomocí metody DFT.

Kombinací teoretického výpočtu metodou DFT a experimentálního měření jsme poukázali na společné rysy a na rozdíly ve fragmentačním schématu všech tří molekul. Navrhli jsme odštěpení dvou vodíkových atomů během plazmově indukovaného fragmentačního procesu. Vodíky mohou být odštěpeny pomocí dvou mechanismů: i. odštěpení dvou vodíků jeden po druhém a ii. odštěpení molekuly H_2 v jednom kroku. Z profilů energie dokážeme určit, který mechanismus bude v tom konkrétním případě pravděpodobnější. Předpokládaný mechanismus je v korelaci s experimentálními výsledky fragmentace zjištěnými z hmotnostních spekter.

KEYWORDS

Ab initio, fragmentation energy, Hartree-Fock, density functional theory, geometry optimization, electron impact ionization, mass spectrometry, ionization energy, appearance energy, bond dissociation energy.

KLÍČOVÉ SLOVA

Ab initio, fragmentační energie, Hartree-Fock, density functional theory, optimalizace geometrie, ionizace nárazem elektronu, hmotnostní spektrometrie, ionizační energie, prahová energie vzniku, disociační energie vazby.

CONTENT

1	INTRODUCTION.....	5
2	LITERATURE REVIEW.....	6
2.1	Fragmentation energy	6
2.1.1	Experimental determination	6
2.1.2	Mechanism of fragmentation	7
2.1.3	Theoretical description.....	8
2.2	Quantum Chemical Methods	9
2.2.1	Born-Oppenheimer approximation	9
2.2.2	Single particle approximation (Hartree-Fock)	10
2.2.3	Linear combination of atomic orbitals (LCAO).....	10
2.2.4	Post-Hartree-Fock methods.....	10
2.2.5	Multi-configuration self-consistent field methods	11
2.2.6	Density functional theory.....	12
2.2.7	Current state of the art.....	12
2.3	Setting of the model.....	13
2.4	Fragmentation in plasma	14
2.5	Fragmentation of organosilicon compounds.....	14
3	METHODS AND MODELS	16
3.1	<i>Ab initio</i> simulation.....	16
3.2	Electron impact ionization	16
3.3	Mass spectra experiments	18
3.4	Relative cross sections experiments.....	18
4	RESULTS AND DISCUSSION	19
4.1	Quantum chemistry computations of simple molecule (propane)	19
4.1.1	The choice of computational method.....	19
4.1.2	The choice of basis set	22
4.1.3	Potential energy surface for propane molecule.....	23
4.2	Analysis of complex compounds (organosilicones)	24
4.2.1	Mass spectra.....	24
4.2.2	Cross sections.....	26
4.2.3	Density functional theory (DFT) calculations.....	27
4.3	Fragmentation mechanism of organosilicones.....	27
4.3.1	Ionization	27
4.3.2	Primary bond cleavage.....	28
4.3.3	Consequent fragmentation-subtraction of hydrogen.....	33
4.3.3.1	Cationic fragmentation mechanism.....	33
4.3.3.2	New approach to the fragmentation	36
5	FINAL CONCLUSIONS.....	39
6	REFERENCES.....	40
7	CURRICULUM VITAE.....	44

1 Introduction

Fragmentation is a process where a large molecule is separated into small molecules. In framework of this thesis, the fragmentation in plasma was investigated using *ab initio* models. The fragmentation is frequently applied for example to the analysis of DNA, where the product of fragmentation can give picture about its structure. DNA fragmentation can be caused by breaking of free radical-induced. Therefore, there is possibility to analyze the fragmentation products of such molecules [1]. Medically, this analysis of DNA fragments can give information about the human fertility [2].

The fragmentation procedures in the gas phase that are driven by electrons are essential to realize the different plasma processes. These processes are widely used in contemporary technologies [3, 4]. By this way, there is possible for example to prepare new polymeric materials that are non-classical. Precursors for these polymers do not contain any double chemical bonds. These properties are strongly dependent on the fragmentation of these precursors.

The calculation of fragmentation energy is very useful, because there is experimentally an ability to change relatively simply the electron energy and thus the creation of different fragment can be optimized. The fragmentation energy can give information about the population of different radicals resulting from the fragmentation. The population analysis can be used as input parameter to investigate the products of subsequent reactions leading to fragmentation. Further, the fragmentation energy can be used as an input property to reflect the chemical reactivity of compound, and it will be possible to study the processes of adsorption and desorption of the resulting radicals or fragments near of some catalyst. This is the reason why our research is focused on the fragmentation energy.

The main goal of the thesis is an analysis of fragmentation process using quantum mechanical methods. A literature review on fragmentation energy and quantum chemical methods will be carried out. The propane will be used as an example of simple molecules for testing of fragmentation analysis. The methylphenylsilane, dimethylphenylsilane and trimethylphenylsilane will be used as an example of complex molecules. The calculation of simple molecule will be used for optimization methods of calculation: selection of optimal method, basis set. The fragmentation energy of complex organosilicon molecules will be calculated. The fragmentation energy will be verified by the positive ion mass spectra and relative partial cross sections obtained experimentally. The individual steps of fragmentation mechanism will be analyzed: electron impact ionization and bond dissociation.

2 Literature review

Ab initio quantum chemistry methods have been previously used to predict the fragmentation energy of large molecules. More recently, the EII technique is used to explain ionic chemistry [5] and energies of fragmentation products [6]. The resulting fragmentation energies are completed with chemical kinetics model. This can give more reasonable results of final concentrations of fragments.

2.1 Fragmentation energy

Fragmentation energy is the property of molecular structure and it is defined as the required energy for separation of several chemical bonds of the large molecule and getting smaller particles (fragments). Fragmentation energy was investigated by using the experiment and also some examples of theoretical calculations by quantum chemical methods.

2.1.1 Experimental determination

There are several experimental techniques describing the fragmentation process such as photoionization [7], collision resilience experiment [8], electron impact ionization [9], mass spectrometry [10], Collision-induced dissociation [11], electron-capture dissociation [12], and electron-transfer dissociation [13]. In all techniques of fragmentation, the principle of fragmentation energy measurement depends on the determination of energies for reactants and products of fragmentation reaction. Then, the fragmentation energy is determined as the difference between the energies of products and reactants.

Experimentally, electron impact ionization and mass spectrometry were selected to describe the fragmentation process. The EII technique is advantageous because it helps to measure the relative ionization energy of the original neutral molecule and appearance energy of the ionic fragments. Ionization energy is the minimum electron energy required to produce molecular ion. Appearance energy is the minimum electron energy necessary to produce a given ionic fragment. The mass spectrum of the original neutral molecule can be obtained in addition; the fragmentation process gives information about the structure and molecular weight of the molecule. The comparison between the experimental data and *ab initio* calculations can be investigated.

S. Denifl et al. [14] determined experimentally appearance energy for some cations of neutral propane formed by the EII experiment at two different gas temperatures (290 K and 690 K). They observed that the appearance energy values were decreased when the gas temperature was increased. They also verified their calculations using high level quantum chemical methods. They used Gaussian-3 theory (G3 theory) [15], Gaussian-3 theory using density functional theory B3LYP (G3B3) [16], and complete basis set-quadratic Becke 3 (CBS-QB3) method [17]. Firstly, they used these three methods to calculate the appearance energy at the gas temperature 290 K where the results were very close from each other. Secondly, they used CBS-QB3 method

to calculate the appearance energy at 290 K and 690 K of gas temperature where their appearance energy was in excellent agreement with experimental data.

J. Kočišek et al. [6] studied the EII technique using crossed electron-molecular beams experiment to investigate the fragmentation of the DMPS molecule. The appearance energies of selected ion fragments were estimated in addition to the ionization energy of the DMPS molecule. They calculated the bond dissociation energy for single bond cleavage as a difference between the appearance energy of the ionic fragment and the ionization energy of the DMPS [18]. They have found that the dissociation energy of methyl group in DMPS⁺ was in a good agreement with theoretical calculations of the DFT methods performed by Choe [19]. They found the same results of dissociation energy for other bonds of the DMPS⁺ except of $m/z = 78$ assigned to C₆H₆⁺.

Mass spectrometry is a standard analytical method. In this technique, molecule is converted into ions and fragments. Then, the composition of molecule and characteristics of fragmentation products like mass-to-charge ratio can be determined. Many experimental studies have been performed to study the fragmentation of fullerenes in neutral and charged C₆₀ [20, 21], C₇₀ [22], and metallofullerenes [23-25]. In particular, these studies revealed that fullerenes sequentially lose C₂ fragments from their cages as is shown in the following reaction:



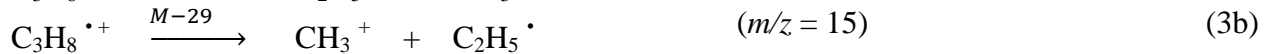
The C₂ fragmentation energy for fullerenes can be determined experimentally using the mass spectrometry technique. Using this technique, it was demonstrated that the C₂ binding energy of C₆₀ lies in the range (7-8) eV [21].

2.1.2 Mechanism of fragmentation

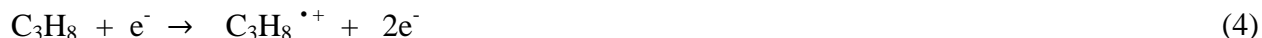
Fragmentation mechanism of propane was investigated using mass spectrometry and EII experiments. According to mass spectrometry technique, butane [10] fragments as follows



According to the fragmentation mechanism for butane, we proposed the detailed mechanism for propane fragmentation.



The EII technique of propane [14] can result the following ionization reactions.



The mass spectra of the propane [26] and butane [27] molecules were presented in literature. These mass spectra are in accord with the proposed mechanism.

2.1.3 Theoretical description

Theoretical description of fragmentation process was investigated by *ab initio* quantum chemistry methods and DFT calculations. E. Vašeková et al. [28] calculated the appearance energy for some cations of neutral ethane using high level *ab initio* quantum chemical methods. They used CBS-QB3 method [15] to calculate the appearance energy of cations of ethane at 293 K and 693 K of gas temperature. The theoretical shift of the appearance energy between these two temperatures was 0.31 eV and was in reasonable agreement with the experimental value.

V. Brites et al. [5] calculated the ionization energy of the DMPS⁺ dimethylphenylsilane cation that is one of the fragmentation products of tetravinylsilane formed by the EII technique using the second-order Møller-Plesset perturbation theory (MP2/cc-pVDZ) level of theory. The ionization energy was about 8.91 eV, which was in excellent agreement with the experimental value of (8.92 ± 0.15) eV of Gaidis et al. [29].

S. T. Nakagawa et al. [30] studied the dissociation of small boron clusters. They calculated the ionization potential energy by using the collision of small boron clusters with Xe atoms at low collision energy (<10 eV). The used methods to carry out this calculation were the DFT(B3LYP) calculation and *ab initio* methods such as HF, MP2, MP4, configuration interaction with single excitation (CIS), and configuration interaction with single and double excitations (CISD). In the comparison to experimental data, they found that the results of the DFT calculations were more accurate than *ab initio* methods that they used and the previous *ab initio* methods [31-33]. The dissociation of clusters by using the collision with Xe atoms is advantageous for calculation of fragmentation energy because it gives better results when the method and basis set are properly selected.

G. A. Dolgonos et al. [34] calculated the C₂ fragmentation energy of C₈₀ using *ab initio* (HF/STO-3G) and the DFT (B3LYP/3-21G) calculations. The C₂ fragmentation energies were calculated as the difference between the C₈₀ isomer energy and the sum of the C₇₈ and C₂ product energies. They found that the DFT methods were more reliable than *ab initio* (HF/STO-3G),

where the calculated C₂ fragmentation energies were in the range (8.7-9.0) eV and in very good agreement with the experimental value of (9.4 ± 0.7) eV.

W. C. Eckhoff et al. [35] calculated the C₂ fragmentation energy of C₇₀ fullerene (C₇₀ → C₆₈ + C₂) using *ab initio* Hartree-Fock (SCF/DZ) and the DFT (BLYP/DZ) calculations. Using the Hartree-Fock (HF) method, the energy of C₂ dissociation from this fullerene was 13.2 eV. The best prediction for the C₂ fragmentation energy of C₇₀ was 11.5 eV by using the DFT method. These results were in sharp disagreement with the majority of the experimental studies.

A. D. Boese et al. calculated the dissociation energy of the reaction C₆₀ → C₅₈ + C₂ using the DFT and MP2 calculations [36]. They found that the fragmentation energy was around (10-11) eV in agreement with the theoretical values of the dissociation energy (11-12) eV [37-40] and with experimental studies (10.5-10.9) eV [41, 42].

2.2 Quantum Chemical Methods

The electronic structure of materials is described by wavefunction (Ψ), which has a meaning square root of the electron density. The function is determined by Schrödinger's equation [1926] (SE) [43]. The exact solution of SE is complex for many compounds. Therefore, several approximations are applied. First example is Wentzel–Kramers–Brillouin, which is used for semiclassical calculation in quantum mechanics. It is suitable for solution of one-dimensional problems. Next class of approximation methods is variational principles or perturbation theories [44].

Ab initio method is used to calculate the electronic structure of the chemical system. In *ab initio* method, the Schrödinger's equation is solved using a basis set. The basis set is a set of functions which are combined in linear combinations to create molecular orbitals. Some physical properties can be determined by *ab initio* electronic structure calculations, i.e. from fundamental quantum theory [45]. The main use of the *ab initio* method is limited to the properties, which depend on electron structure such as molecular geometries, total energy, ionization energy, electron affinity, appearance energy, bond dissociation energy, dissociation energy, potential energy surfaces (PES), vibrational frequencies, dipole moment, and charge distribution.

The Schrödinger's equation can be written in form:

$$\mathbf{H}_{mol} \Psi = E \Psi \quad (5)$$

Where E is the total energy of the system, Ψ is the wavefunction which is a function of the positions of the electrons and the nuclei within the molecule, and \mathbf{H}_{mol} is the molecular Hamiltonian of a system which describes a many body system consisting of nuclei and electrons.

2.2.1 Born-Oppenheimer approximation

Ab initio method is based on the Born–Oppenheimer (BO) approximation. It assumes that the electron properties only must be considered in calculation. Wavefunctions of atomic cores are simplified and their kinetic energy is treated to be zero [46].

2.2.2 Single particle approximation (Hartree-Fock)

For more complicated systems, the HF approach is applied [47]. This method does not include the full treatment of the effects of electron correlation where the coulombic repulsion between two electrons is not explicitly considered but its average effect is included in the calculation. This means that each electron in a molecule moves in an average electric field generated by all of the other electrons.

For the system containing only one electron, the Schrödinger's equation can be exactly solved. The HF method is variational method, meaning that the energies predicted by this method are always equal to or greater than the real energy resulting from the exact solution of the Schrödinger's equation [48]. The HF method is suitable to compute the structures, vibrational frequencies of stable molecules [46]. In addition, excited states are difficult to calculate using the HF theory [49].

2.2.3 Linear combination of atomic orbitals (LCAO)

This approximation involves expressing the molecular orbitals as linear combinations of basis functions. These basis functions are usually identified with atomic orbitals. An individual molecular orbital is defined as

$$\psi_i(\mathbf{r}) = \sum_{s=1}^m c_{si} \Phi_s(\mathbf{r}) \quad i = 1, 2, 3, \dots, m \text{ (component MOs)} \quad (6)$$

Where ψ_i is the molecular orbital i , c_{si} is the expansion coefficient of the atomic orbital s in the molecular orbital i , Φ_s is the atomic orbital s , and m is the number of atomic orbitals. This approximation is usually called the linear combination of atomic orbitals (LCAO) approach that leads to linear equation for the coefficients of the molecular orbitals [50].

2.2.4 Post-Hartree-Fock methods

As mentioned in the previous section, the HF method neglects the correlated motion of electrons resulting from Coulombic interactions. The difference between the HF and exact (nonrelativistic) energies is the correlation energy,

$$E(\text{exact}) = E(\text{Hartree-Fock}) - E(\text{correlation}) \quad (7)$$

The neglect of correlation between opposite spins electrons leads to deficiencies in the description of electronic structure and some clearly anomalous results [51, 52]. Therefore, other theoretical methods, which take into account effects of spin electron correlation, have been developed. The electron correlation describes the energy contributions resulting from the interaction between the motions of different electrons in the electronic structure. Such methods are referred to as post-Hartree-Fock methods because they add correlation corrections to the HF method. There are various post-Hartree-Fock methods such as Møller-Plesset perturbation theory MPn, configuration interaction (CI), coupled cluster (CC) methods. Post-Hartree-Fock methods

provide accurate treatment of the structures and energies of molecules, but they differ in computational costs [53].

Møller-Plesset perturbation theory (MP n), where n is the order of the perturbation, is a method to compute the correlation energy using the many-body perturbation theory [54, 55]. The principle of perturbation theory is that the system is subjected to external potential (perturbation) such as a magnetic field or electromagnetic radiation relative to the internal HF potential in which the electrons are moving. Then the system of interest is perturbed or changed slightly from a system whereby the mathematical solution is known (is solved exactly or approximately). There are several levels of MP energy such as MP0, MP1, MP2, etc.

The advantage of many-body perturbation theory is that it is size-consistent in the sense that for two widely-separated fragments, the energy obtained using this method equals to the sum of the energies of these two fragments computed separately, however, it is not variational [56].

In the CI calculation, the electron correlation is treated [57]. On the other hand, the HF calculation is performed to result the occupied MOs (corresponding to the HF determinant), then the excited Slater determinants are generated by replacing one or more occupied orbitals with unoccupied (virtual) orbitals of higher energy. The total wavefunction is written as a linear combination of determinants (HF determinant and excited Slater determinants) with the molecular orbital expansion coefficients that can be determined when the energy is minimal (or at least stationary). According to the number of occupied HF MOs that can be exchanged by unoccupied MOs, The excited states are single (S), double (D), triple (T), and quadruple (Q). Therefore, there are several variants of the CI method such as CIS, CID, CISD, and CISDT [58, 59].

The CC method is similar to the CI calculation, where the total wavefunction is as a sum of the HF ground state determinant and determinants representing the transmission of electrons from HF determinant to virtual MOs. In the CC calculation, the selection of determinants is more difficult than selection them in a CI method [60]. The CC theory [61-63] takes into account electron correlation. In the CC method, excitations are also included in calculation, for example double excitations (D) in CCD [64], single (S) and (D) excitations in CCSD [65], and S, D, and T excitations in CCSD(T) [66]. All CC methods are size-consistent [67]. However, CC methods are not variational [68].

2.2.5 Multi-configuration self-consistent field methods

In previous section, the wavefunction of system was represented starting from a single HF determinant with occupied bonding orbitals (HOMO orbitals). Multi-configuration self-consistent field (MCSCF) method uses more than one configuration (HF determinant) to describe the total wavefunction. In MCSCF method, bonding and antibonding orbitals are treated to yield configurations. The consideration of antibonding orbitals is very important to study the dissociation of the molecule with stretched bond lengths where the energy gap is very small. Both the coefficients of the configurations that are in front of the determinants and the MOs used for constructing the determinants are optimized by the variational principle [69].

There is developed type of MCSCF calculation called complete active space self-consistent field approach (CASSCF) [70] used to study chemical reactions and to calculate electronic spectra. In this approach, very large numbers of configurations are included in the calculation [71] by dividing the molecular orbitals into three sets: inactive orbitals, virtual orbitals, and active orbitals.

2.2.6 Density functional theory

The DFT calculation [72, 73] was developed by Hohenberg and Kohn (1964) and by Kohn and Sham (1965). The DFT method is an alternative to *ab initio* methods. The difference between this method and *ab initio* method is that the energy of the molecule can be determined in the DFT method from the electron density while from the wavefunction in *ab initio* method. In the DFT methods [74], electron correlation effects are taken into account and the exchange-correlation energy is computed using functional of the electron density. Functional is a function defined by another function. There are a variety of functionals used in the DFT methods such as Becke style three parameters [75] density functional method with the Lee-Yang-Parr correlation functional (B3LYP) and Becke style three parameters density functional method with the Perdew-Wang (B3PW91) [76]. Correlation functional (B3LYP) is very popular. In our case, each single function represents electron density of one atom. Using the functional, the electronic energy can be divided via the Kohn-Sham equations [77] into several terms which are computed separately. These items are the kinetic energy resulting from the motion of the electrons, the potential energy of nuclear-electron interaction and nuclear-nuclear repulsion, the electron-electron repulsion, and the exchange-correlation that represents the quantum mechanical exchange energy and the dynamic correlation energy.

2.2.7 Current state of the art

For many-body system, *ab initio* method requires to find a solution of the Schrödinger's equation. So far, there is no exact solution of the Schrödinger's equation, but by using some approximations, the physical properties, electronic structure, and total energy of molecule can be calculated. The PES and the HOMO and LUMO energies and their energy gap were selected. The PES is a concept used in computational chemistry to represent the relation between the energy of the system and its geometry. On this PES, minima and saddle points can be characterized.

Minima are observed at equilibrium structures and correspond to optimized geometries, and saddle points correspond to a transition structure of the system. The HOMO and LUMO energies and their energy gap reflect the chemical reactivity and kinetic stability of the system. When the energy gap is large, the system is less reactive and not kinetically stable, and when the energy gap is small, the system is more reactive and kinetically stable. These are the reasons why the calculations of the PES, HOMO energy, and LUMO energy were selected.

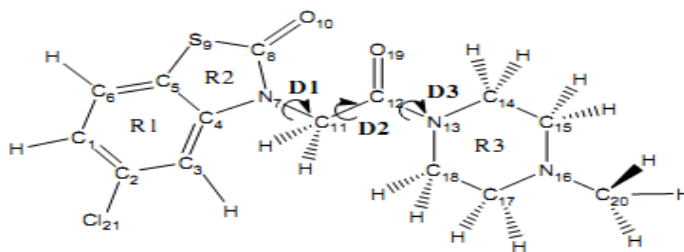


Figure 1. 5-chloro-3-(2-(4-methylpiperazin-1-yl)-2-oxo-ethyl)benzo[d]thiazol-2(3H)-one (5CMOT) [78].

As example of the PES is a work of E. Tasar et al. [78]. The studied molecule was 5-chloro-3-(2-(4-methylpiperazin-1-yl)-2-oxo-ethyl) benzo[d] thiazol-2(3H)-one molecule (abbreviated as 5CMOT). The schematic depiction of 5CMOT is shown in Figure 1. They used the DFT(B3LYP) method with 6-31G(d) to calculate the PES. They found that the 5CMOT molecule has three different conformers. There was one conformer that has stable structure corresponding to the lowest energy value (local minimum) on the PES graphs. They also calculated vibrational spectra of the most stable structure using the DFT(B3LYP) and *ab initio* HF methods. The results of the DFT methods were in an agreement with the experimental data.

As example of the HOMO energy, LUMO energy, and LUMO-HOMO energy gap is a work of R. J. Xavier et al. [79]. For this calculation, they used the HF and DFT(B3LYP) methods with 6-311++G(d, p) basis set. It was found that the DFT(B3LYP) method gives a lower energy gap in comparison with the HF method. The calculation of energy gap between HOMO and LUMO orbitals is good to get information about the chemical reactivity of the molecule where the lower value of this energy implies that the system is more reactive and kinetically stable and its electrons can more easily be excited. Recently this energy gap is used to prove the bioactivity from intermolecular charge transfer [80, 81].

2.3 Setting of the model

Here, basis set is used. Basis set is the set of mathematical functions used to describe the molecular orbitals within a molecule. There are several types of basis sets such as minimal basis set, split valence basis set, polarized basis set, and diffuse basis set. Minimal basis sets contain the minimum number of basis functions and they are used for very large molecules. The most popular minimal basis set is the STO-3G basis set [46]. Split valence basis sets allow orbitals to change size by increasing the number of basis functions of the same angular type (secondary quantum number) per atom. Split valence basis set can be double or triple according to the number of sizes of basis functions for each valence orbital. For example, double zeta basis set 3-21G uses two sizes of basis functions for each valence orbital, while triple split valence basis set 6-311G uses three sizes of basis functions [50]. Polarized basis sets are the modified form of split valence basis sets. These Polarized basis sets allow orbitals to change shape by adding basis functions (orbitals) with higher angular momentum. In polarized basis set, d functions are added to heavy atoms (all atoms, except hydrogen atoms), p functions are added to hydrogen atoms,

and f functions are added to transition metals. Polarized basis sets can be characterized by adding one or two asterisks. The 6-31G* and 6-31G** are examples of this type of basis sets [60]. Diffusion basis sets are more developed form of polarized basis sets. These basis sets allow orbitals to occupy a larger region of space by adding highly diffuse functions to atoms. Here, one or two plus signs are added. The 6-31+G* and 6-31++G* are examples of diffusion basis sets [46].

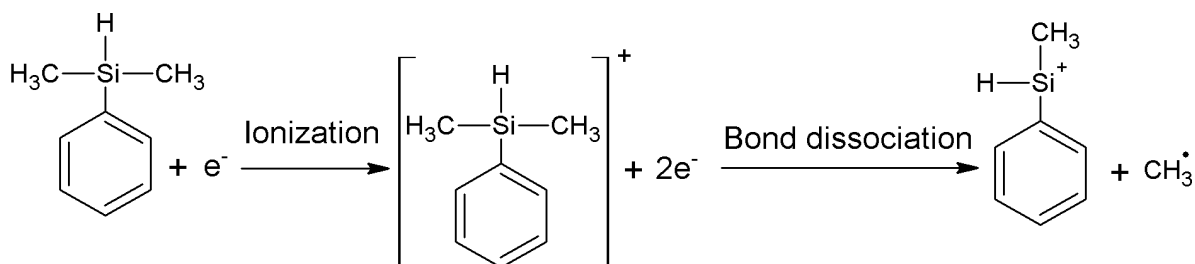
2.4 Fragmentation in plasma

Chemical vapor deposition technique has been used for thin film production for more than 50 years. Main applications of organosilicon precursors are in microelectronics [82], automotive and food industry [83]. During 1980's, this deposition technique has been improved by adding plasma to the process. Plasma enhanced chemical vapor deposition (PECVD) or plasma assisted chemical vapor deposition (PACVD) allow using many new types of precursors, especially organosilicones. For example, the MPS molecule can be used as a compatibilization agent. The plasma deposition is accompanied by fragmentation of molecule. The composition of fragments is important parameter for reactivity of inorganic surface. These precursors offer several advantages. Organic groups have nearly infinite options for proper control of deposited layers. Additionally, they are compatible with other organic compounds and provide elasticity, preventing the layer to crack. Silicon atoms support binding of organic, polymers and biomaterials to inorganic substrates including glass, or ceramics. In that case the bio- or organic phase must be attached to inorganic surface in controlled way [84]. Hexamethyldisiloxane (HMDSO) and tetraethyl orthosilicate (TEOS) are used as PECVD precursors very often [85].

2.5 Fragmentation of organosilicon compounds

The organosilicone molecules play a key role in plasma physical chemistry [86, 87]. However, they can be applied also for the understanding of fragmentation process. The understanding of structure-properties relations can be highlighted by the cases, which are structurally similar and have different response. Fragmentation of organosilicones by electron impact is the critical point with respect to plasma based CVD techniques. The presented study deals for the investigation of the role of organic content in organosilicones that differ by number of CH₃ functional groups in their structure. Particularly, we would like to find relation between primary chemical structure and fragmentation properties of the MPS, DMPS, and TMPS compounds. These three molecules have similar structure, however, their electron fragmentation products according to the mass spectra proved to be significantly different. The reason is probably that the detailed individual mechanisms may be specific for such three molecules. We found, that some reactions show common features. For example subtraction of two hydrogens from molecule runs sometimes step-by-step and in other cases it runs irregularly. The mechanism in two variants is present for all molecules. We believe that some reactions can be observed in general in the mechanism independently on molecule. We combine the quantum chemical simulations and experimental technique (mass spectra of fragments obtained by monochromatic

electron impact) in order to find the most important reactions causing specific for the fragmented molecule. In general, the molecular ions are not too stable under electron impact and they rapidly form various fragments. The process after the ionization depends on the energy profile of bond dissociation. The phenylsilane dissociation by the EII technique was described in the literature as typical example of similar compounds [88, 89]. The organosilicon molecules are also interesting from theoretical point of view. The silicon as a central atom has more complex electron orbitals than carbon atom in analogous molecules, and the C-Si bond is covalent. Some aspects of their fragmentation process are presented in literature. The fragmentation mechanism of the DMPS molecule shown by Scheme 1 was proposed [6].



Scheme 1. Scheme of dimethylphenylsilane fragmentation process: Phase 1: electron induced ionization; Phase 2: bond dissociation; in Scheme is only example; in reality, the fragmentations can run in several ways according to the bond being cleaved [6].

The mechanism presented in Scheme 1 is as an example of one dissociation reaction for the DMPS molecule. However, the second phase, bond dissociation, can vary for different molecules. There can be large combination of the bonds being dissociated. We have investigated the fragmentation process initialized by the EII technique experimentally by mass spectra and theoretically by quantum chemistry calculations (DFT method). The fragmentation energy in the first approximation is calculated from the energies of fragmentation products and of original molecule [36]. Later the mechanism from Scheme 1 was included also into theoretical models. T. Veszpremi et al. [90] calculated the ionization energy of the TMPS molecule and measured it based on the mass spectrum produced by ultraviolet photoelectron spectroscopy. Choe [19] calculated the dissociation energies required to lose benzene from the phenylsilane derivatives (except for TMPS molecule). The DFT calculations showed that the increase of methyl substituents at the silicon atom made the dissociation process easier.

3 Methods and models

Firstly, energies of molecule and its fragments are calculated using MOLPRO software. Secondly, these energies are applied to kinetic description of molecule fragmentation process.

3.1 *Ab initio* simulation

First of all, we need to set up MOLPRO program [91] that is an *ab initio* software package, which serves for calculating the molecular electronic structure by quantum chemical methods. Then, it is necessary to write and prepare input file that contains some information about the molecule (geometry of molecule), computational method, and basis set.

3.2 Electron impact ionization

The fragmentation process can also be described experimentally. It was investigated the EII experiment for the MPS, DMPS and TMPS compounds using the mass spectrometry technique. The composition of fragmentation products from MPS and TMPS measured by this EII experiment is interpreted with respect to the ionization energy, appearance energies of fragments and bond dissociation energy of selected bonds. The results are compared to the previously published experimental data for DMPS molecule. Comparison with the theoretical bond dissociation energies calculated using the DFT calculations is presented.

We describe the mechanism, where the bond dissociation is preceded by the EII experiment while radical-ion appears. The radical ion can be subject of three types of fragmentation reactions: cleavage of σ bond, cleavage of two σ bonds, and cleavage with complex rearrangements [92]. The cleavage of single bonds can run serially. In some cases, the cleavage of bonds in the original molecule can be followed by destruction into fragments.

The complete description of the process needs many parameters such as ionization energies, appearance energy, and heats of formation. All the parameters must be known for the many radicals and ions. Some of the parameters (i.e. appearance energy, ionization energy) and mass spectra were presented in literature (Gaidis et al. [29], Dube et al. [93], Kuritka et al. [94], Kočišek et al. [6]).

The EII technique is the classical ionization method used in mass spectroscopy. By the EII reaction of molecule, the nature of fragmentation products formed can be assigned. The EII reaction can be expressed by the following equation:



where M^+ is the molecular ion that can have a stable form or may be subject of fragmentation or isomerization. The fragmentation products may be either fragment ions or radicals.

We have measured the electron ionization of methylphenylsilane (molecular weight 122.24 g/mol) and trimethylphenylsilane (molecular weight 150.29 g/mol) molecules. Both samples are liquids and were obtained from Sigma-Aldrichs with high purity ($\geq 98\%$ for MPS and $\geq 99\%$ for TMPS). The electron impact experiments were done using the crossed electron-molecule beam apparatus. The apparatus was described in detail in the work of Stano et al [95]. A schematic view of the main parts is shown in Figure 2.

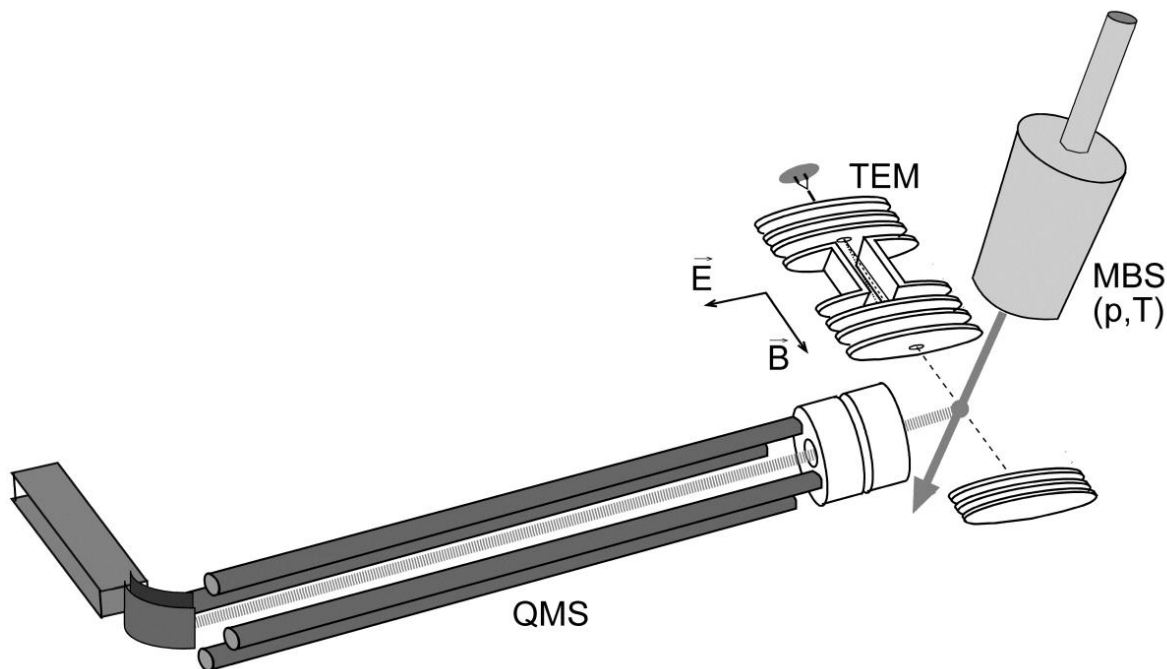


Figure 2. Schematic view of the apparatus. TEM- trochoidal electron monochromator, (QMS)- quadrupole mass spectrometer, MBS- molecular beam source, E- homogenous electric field, B- homogenous magnetic field [95].

The electron beam is formed by a trochoidal electron monochromator (TEM), where the electron energy resolution of the electron beam in present experimental study was 300 meV. The molecular beam is formed in the molecular beam source (MBS) by effusion of gas phase MPS/TMPS samples through a capillary (0.5 mm diameter and 4 mm long) into the reaction chamber. The temperature of the molecular beam source was ~ 300 K, and the pressure can be varied in the range (1-10) Pa. The molecular beam crosses perpendicularly the electron beam. Due to a weak electric field, the ions formed in the intersection volume are extracted into quadrupole mass spectrometer (QMS), where these ions can be analyzed. The calibration of the electron energy scale for the measured ion efficiency curves was carried out using the ionization energy for the reaction $\text{Ar} + e^- \rightarrow \text{Ar}^+ + 2e^-$ with an ionization energy of (15.759 ± 0.001) eV

[96]. In our experimental study, we used two basic modes of operation. The first one is mass spectra, and the second mode is relative cross sections.

3.3 Mass spectra experiments

In this experiment, the standard mass spectra (relative abundances of the m/z products) for the MPS and TMPS compounds were recorded at constant electron energy of 70 eV. The mass spectrum of DMPS was taken from literature [6]. These mass spectra reflect the composition of molecule and give us the overview of fragmentation products.

3.4 Relative cross sections experiments

In our experiment, the ion efficiency as function of the incident electron energy (the relative cross section of ion) was measured for fixed m/z mass values. The appearance energies of the molecular ion and the corresponding ionic fragments were evaluated by fitting an expected dependence of ionization cross section on electron energy to a model function based on a Wannier threshold law [97].

$$\sigma(E) = b + a(E - AE)^d \quad (9)$$

Here AE , b , a , d are the variable fitting parameters, σ is an ionization cross section close to the ionization threshold, E represents electron energy, b is the background signal from the detector, a is a scaling factor, and d is an adjustable exponential factor. The fitting procedure is a convolution of the expected cross section and monochromatized electron energy distribution function, which is assumed to be Gaussian function. If there are two ionic states close to the threshold region (the case for the calibration gas Ar^+), other parameters can be added to previous Wannier threshold law.

$$\sigma(E) = b + a_1(E - AE_1)^{d_1} + a_2(E - AE_2)^{d_2} \quad (10)$$

In this case, the fitting procedure contains seven independent variables. Bond dissociation energy ($\text{AB}^+\text{-C}$) can be derived from the ionization (ABC^+) and appearance energy (AB^+) or from two corresponding appearance energies (for $\text{A}^+\text{-B}$) from (AB^+) and (A^+).

In the literature, the fragmentation of simple systems was mostly focused to the study of electron impact phase [98, 99]. The process was studied experimentally and theoretically in order to analyze detailed aspects of the process such as ionization cross section of molecules that is the probability of an ionization process during an electron impact. The experimental description of the process was focused to electron impact cross section of molecule [100, 101]. The electron impact cross-section is efficient part of atom cross-section, where electron can induce ionization and thus it determines the ability of ionization of given molecule or atom. Most of authors describe the cross-section to the charge +1, however, the cross-sections for ionization to the charge +2 and +3 can be measured, too [102]. The cross-section can be calculated theoretically using different theoretical models such as binary encounter dipole (BED) models [103, 104].

4 Results and discussion

Our calculations were performed using quantum chemistry computations, where *ab initio* and DFT calculations were used to compute some chemical properties for selected compounds. MOLPRO program was used to make simulations [91].

4.1 Quantum chemistry computations of simple molecule (propane)

Some selected properties for propane were investigated.

4.1.1 The choice of computational method

Geometry optimization or energy minimization is used in computational chemistry to find the lower energy shape that corresponds to equilibrium structure of molecule (minima on the PES graph). The influence of method was investigated on propane molecule. Geometry optimization was calculated using the same basis set 6-311G(d,p) and different methods such as HF, MP2, MP3 (third-order Møller-Plesset perturbation theory), MP4, CI, QCISD, QCISD(T), CCSD, CCSD(T), multireference configuration interaction (MRCI), and the DFT(B3LYP) method. Predicted results of energy minimization are shown in Figure 3.

Evidently, the DFT(B3LYP) calculation gives the lowest value of energy minimization. On the contrary, the HF calculation results the highest energy minimization. Concerning Møller-Plesset perturbation theory (MP_n) methods, the energy minimization decreases with the increase of the order of the perturbation (n), where MP₂>MP₃>MP₄. Energy minimization using the CI methods decreases with the increase of excitations CI> QCISD>QCISD(T). The CC methods have the same result like in the CI methods, where the energy minimization CCSD>CCSD(T). The CI and MRCI methods have the same exact results. Results of CCSD(T) and QCISD(T) methods are relatively similar.

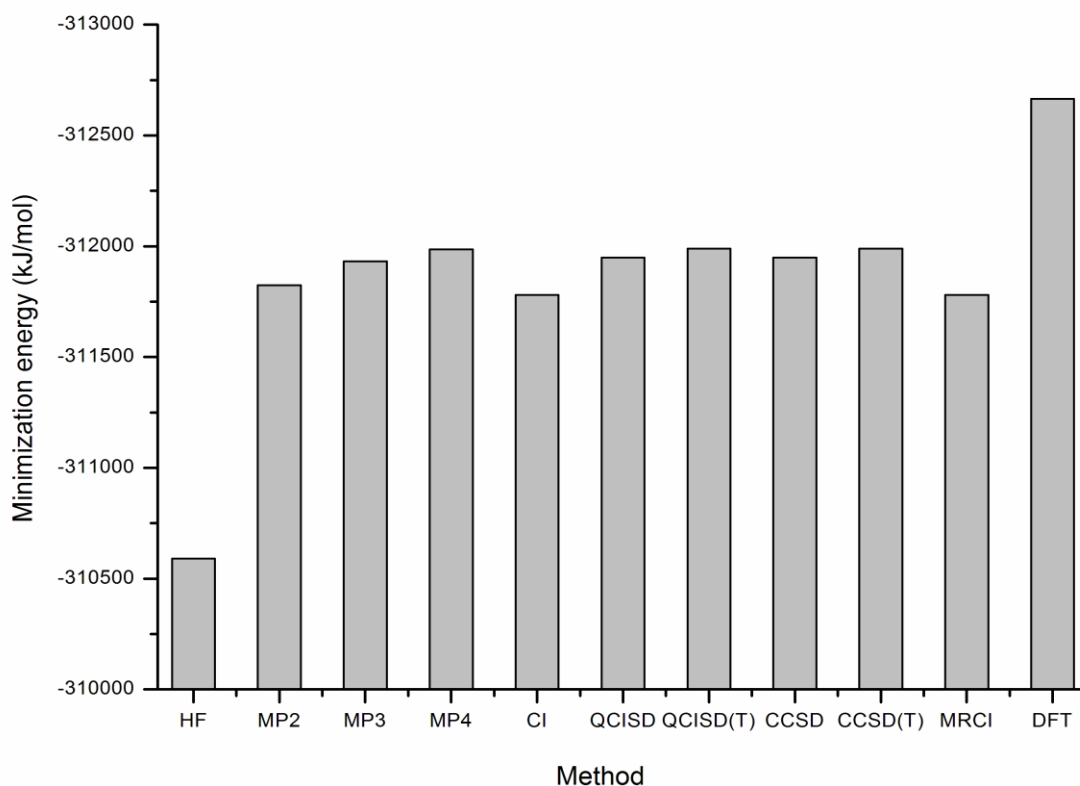


Figure 3. Energy minimization of C_3H_8 using different methods with the same basis set 6-311G(d,p).

Molecular orbitals can be used to explain the distribution of charge and dipole moment for the molecule. The calculations of molecular orbital energies specifically, the HOMO and LUMO energies were performed to determine the energy gap between HOMO and LUMO orbitals. Firstly, molecular orbitals MOs of C_3H_8 molecule were calculated using MOLPRO software [91]. Secondly, molecular orbitals were visualized using visual molecular dynamics (VMD) program [105]. According to this calculation, it has been found that propane molecule has 23 molecular orbitals. The HOMO and LUMO energies were calculated using different methods with the same basis set 6-311G(d,p). From the energy gap between HOMO and LUMO orbitals, wavelengths at which the compound can absorb the light were calculated and compared with maximum absorption of ultraviolet and visible spectra (λ_{max} is approximately equal to 135 nm [106]). The calculated values of HOMO energy, LUMO energy, LUMO-HOMO energy gap, and wavelength of propane are shown in Table 1.

Table 1. HOMO energy, LUMO energy, LUMO-HOMO energy, and wavelength of C₃H₈ molecule calculated using different methods and the same basis set 6-311G(d,p).

Method	HOMO energy (kJ/mol)	LUMO energy (kJ/mol)	LUMO-HOMO energy (kJ/mol)	λ_{\max} (nm)
HF	-1231.73	412.53	1644.26	72.88
MP2	-1228.58	411.39	1639.97	73.07
MP3	-1229.41	411.08	1640.49	73.05
MP4	-1228.33	410.40	1638.73	73.13
CI	-1229.89	412.04	1641.93	72.99
QCISD	-1228.15	410.61	1638.76	73.13
QCISD(T)	-1228.24	410.27	1638.51	73.14
CCSD	-1228.21	410.65	1638.86	73.12
CCSD(T)	-1228.25	410.29	1638.54	73.14
MRCI	-1229.89	412.04	1641.93	72.99
DFT(B,LYP)	-741.64	67.59	809.23	148.09

As can be seen from Table 1, the HF and post-Hartree-Fock methods give relatively similar values of LUMO-HOMO energy gap. The LUMO-HOMO energy gap calculated using the DFT(B,LYP) method is smaller than that of the HF and post-HF methods. The small value of energy gap indicates that the molecule can be easily excited and there is easier decomposition of bond. Wavelengths calculated and measured show that the DFT method achieves more agreement with experiment compared with HF and post-HF methods. The 3D plots of the HOMO orbital, LUMO orbital, and electron density for propane molecule calculated using the DFT(B,LYP)/6-311G(d,p) method are shown in Figure 4.

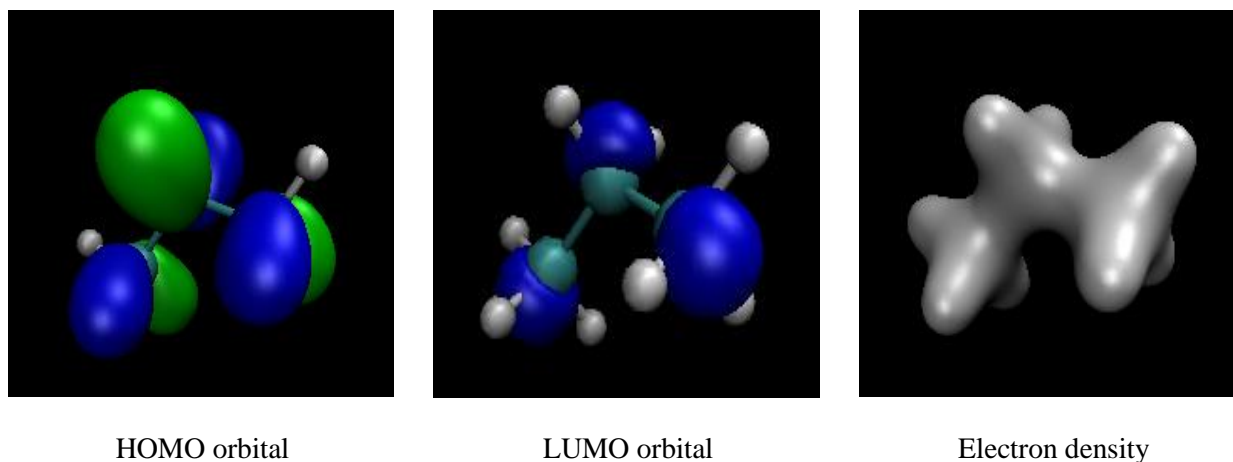


Figure 4. Plots of HOMO orbital, LUMO orbital, and electron density of propane calculated using the DFT(B,LYP)/6-311G(d,p) method.

The ionization energy of propane molecule was calculated using the DFT [RKS, UKS, B3LYP, and (B,LYP)] methods and the same basis set 6-311G(d,p) to test the DFT calculations. Theoretical results of ionization energies were compared with the experimental value (experimental ionization energy of propane is (11.01 ± 0.07) eV [107] and (10.9 ± 0.1) eV [108]). Results of the DFT calculations for propane with 6-311G(d,p) basis set are shown in Table 2.

Table 2. Ionization energy of propane calculated using the DFT methods and 6-311G(d,p) basis set.

Method	C ₃ H ₈ energy (eV)	C ₃ H ₈ ⁺ energy (eV)	Ionization energy (eV)
RKS	-3211.33	-3200.87	10.46
UKS	-3211.33	-3200.88	10.45
B3LYP	-3240.53	-3229.69	10.84
B ₁ LYP	-3240.62	-3230.10	10.52

As shown in Table 2, the ionization energy calculated using the DFT(B3LYP)/6-311G(d,p) method has the best agreement with experiment compared with the other DFT methods.

4.1.2 The choice of basis set

The DFT(B3LYP) calculations with different basis sets were also studied to test the influence of basis set size on ionization energy of propane molecule. Theoretical results of ionization energy were compared with previous experimental data. Predicted results of ionization energy are given in Table 3. The comparison of calculated values of ionization energies with the experimental data shows that the large basis sets give better correlation between theory and experiment in comparison to the small basis sets.

Table 3. Ionization energy of C₃H₈ calculated using the DFT(B3LYP) method and different basis sets.

Basis set	C ₃ H ₈ energy (eV)	C ₃ H ₈ ⁺ energy (eV)	Ionization energy (eV)
STO-3G	-3201.16	-3190.80	10.36
3-21G	-3222.06	-3211.20	10.86
6-21G	-3236.28	-3225.44	10.84
6-31G	-3238.79	-3227.97	10.82
6-311G	-3239.51	-3228.57	10.94
6-31G*	-3239.48	-3228.67	10.81
6-311G*	-3240.24	-3229.35	10.89
6-31G**	-3239.78	-3229.03	10.75
6-311G**	-3240.53	-3229.69	10.84
6-31+G*	-3239.60	-3228.70	10.90
6-31+G**	-3239.88	-3229.05	10.83
6-31++G**	-3239.88	-3229.06	10.82
6-311+G*	-3240.25	-3229.36	10.89
6-311+G**	-3240.54	-3229.70	10.84
6-311++G**	-3240.54	-3229.70	10.84
6-31G(3df,3pd)	-3239.97	-3229.22	10.75
6-311G(2df,2pd)	-3240.77	-3229.95	10.82
6-311G(3df,3pd)	-3240.78	-3229.96	10.82
6-311+G(2d,p)	-3240.61	-3229.78	10.83
6-311+G(2d,2p)	-3240.71	-3229.87	10.84
6-311++G(2d,2p)	-3240.71	-3229.87	10.84
6-311++G(3df,2p)	-3240.74	-3229.91	10.83
6-311++G(3df,3pd)	-3240.79	-3229.96	10.83
VDZ	-3239.53	-3228.83	10.70
VTZ	-3240.85	-3230.03	10.82
VQZ	-3241.10	-3230.27	10.83
V5Z	-3241.18	-3230.35	10.83
aug-cc-pVDZ	-3239.79	-3229.02	10.77
aug-cc-pVTZ	-3240.86	-3230.04	10.82
aug-cc-pVQZ	-3241.11	-3230.28	10.83

4.1.3 Potential energy surface for propane molecule

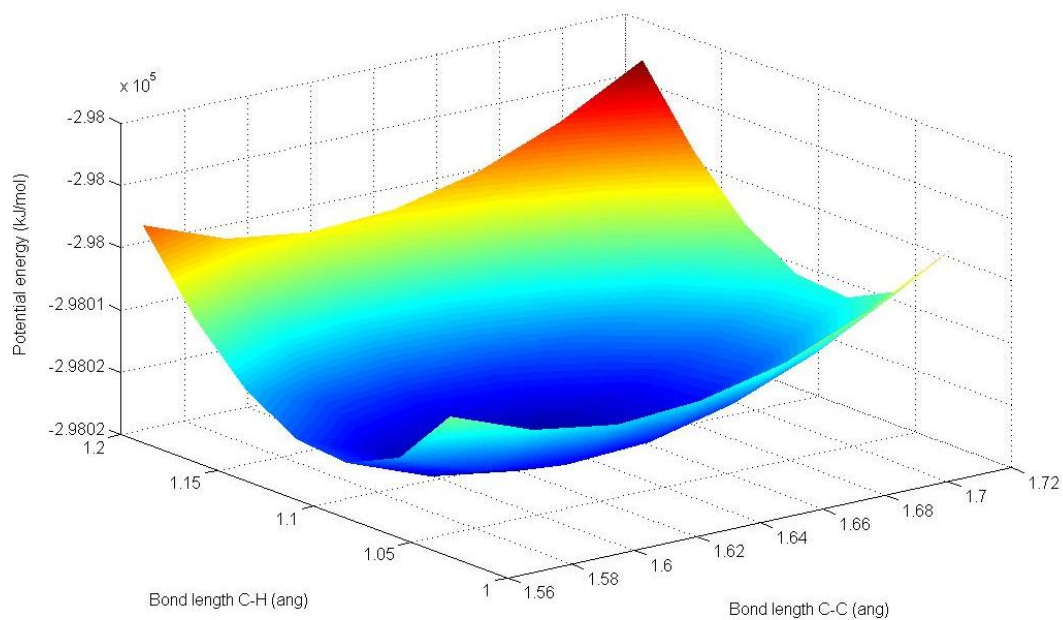


Figure 5. Potential energy surface of electronic ground state of propane using CCSD(T)/6-311G level.

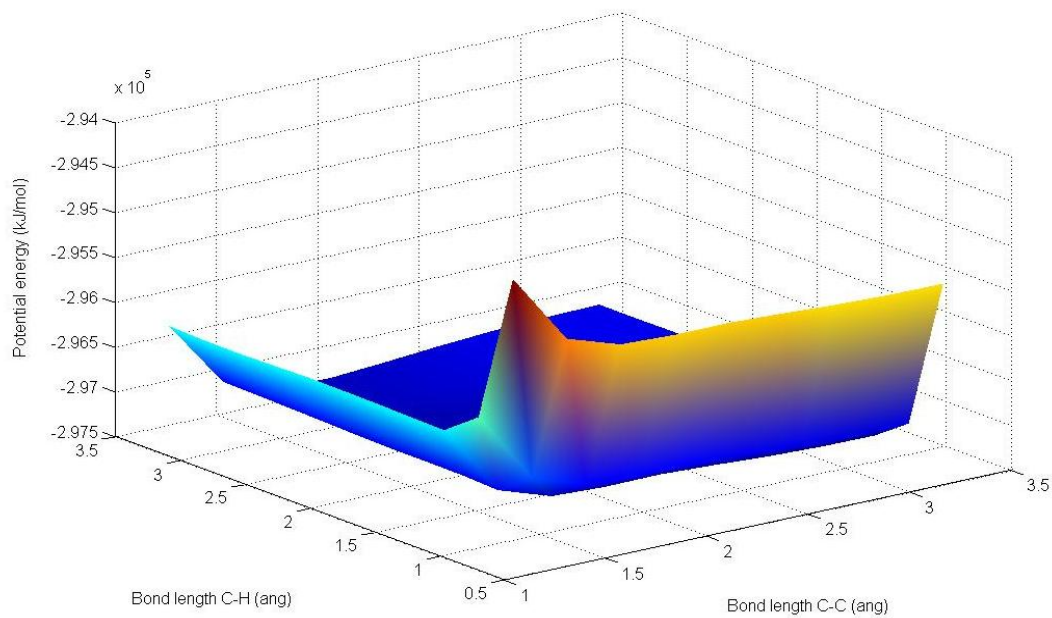


Figure 6. Potential energy surface of electronic excited state of propane using CCSD(T)/6-311G level.

The PES calculations of propane molecule in an electronic ground and excited states were investigated for understanding the relationship between the energy of propane molecule and its structure. This calculation was performed in two steps with considering of two parameters C-H and C-C bond lengths. The first step was the calculation of energies at different geometries by *ab initio* calculations. The second step was the use of calculated energies as input data in MATLAB software to get the PES graphs. The calculation of the PES in the ground and excited states was performed using the CCSD(T)/6-311G level of theory. Figures of PES of propane in ground and excited states are shown in Figures 5 and 6, respectively. Figure 5 explains the minimum energy for C-H and C-C bond lengths that corresponds to the equilibrium structure of molecule. Figure 6 shows that the potential energy of excited state increases when two atoms are approaching from each other, meaning that when the vibration stretching decreases.

4.2 Analysis of complex compounds (organosilicones)

The MPS, DMPS, and TMPS are used as an example of complex compounds.

4.2.1 Mass spectra

Organosilicon compounds such as MPS, DMPS, and TMPS were analyzed by the DFT calculations. The analysis was also supported by electron impact experiment. Electron impact ionization technique was applied to MPS and TMPS compounds to carry out two types of experiments: mass spectrum and relative cross section experiments. The first type of electron impact experiments is the determination of mass spectrum of the sample.

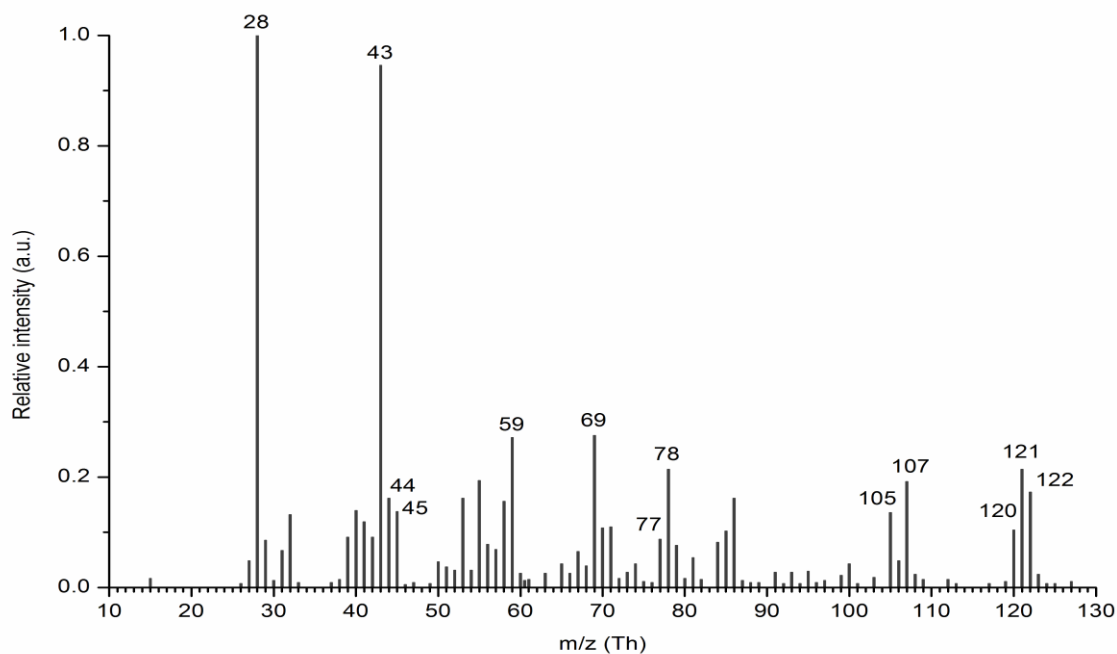


Figure 7. Electron impact mass spectrum of methylphenylsilane at electron energy of 70 eV.

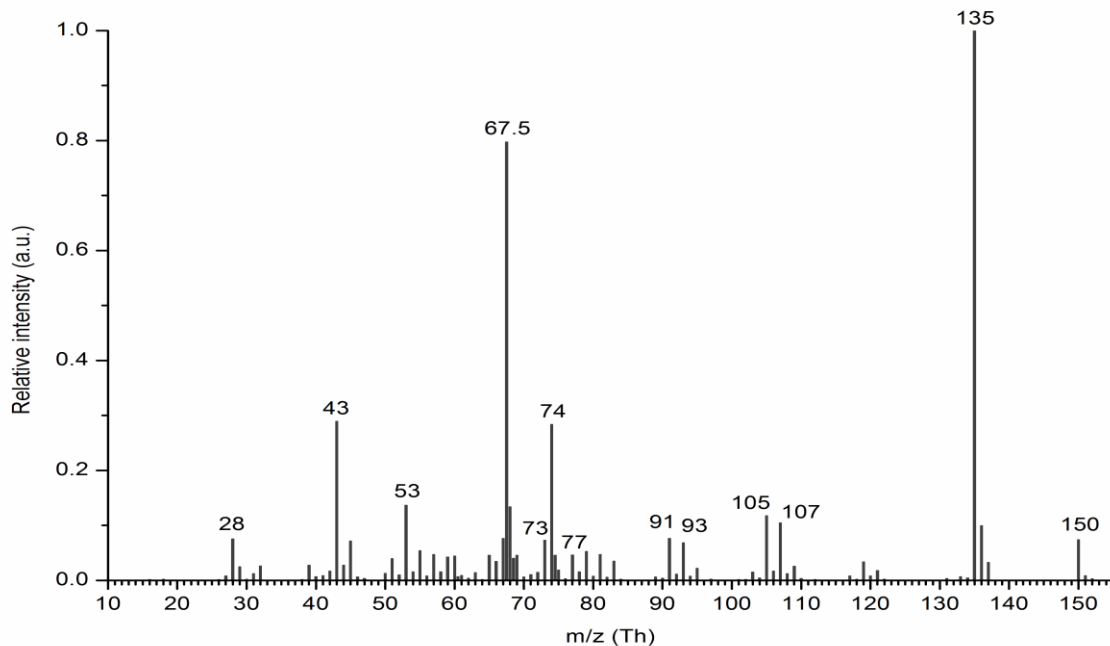


Figure 8. Electron impact mass spectrum of trimethylphenylsilane at electron energy of 70 eV.

The mass spectra of MPS (Figure 7), and TMPS (Figure 8) were measured. They reflect the composition of molecule and give us the overview of fragmentation products. The remaining mass spectrum of DMPS was taken from the work of Kočišek et al. [6], which was measured with similar methodology. We found that the MPS, DMPS, and TMPS compounds have significantly different mass spectra and fragmentation products. The mass spectrum contains general information about all fragmentation products. We cannot assign the products to individual steps in Scheme 1. The mechanism enables the molecule number of combinations of different partial reactions. Each step of fragmentation process was analyzed for each compound (MPS, DMPS and TMPS). In all steps we analyzed, whether the fragmentation of compounds is similar or it is different. The initial hypothesis is, that the spectra are different as the molecules have different number of hydrogens and methyl groups attached to the Si atom. The peaks from mass spectra are summarized in Table 4.

Table 4. The expected ions and their corresponding masses for MPS, DMPS, and TMPS compounds. $m/z - x$ axis of mass spectra; Reaction – origin of fragment: **I** – ionization reaction; **P** – primary bond cleavage; **C** – consecutive reaction; **N** – not known; **DI** – double ionization; **DP** – double ionization with primary bond cleavage.

MPS			DMPS			TMPS		
m/z	Fragment	Reaction	m/z	Fragment	Reaction	m/z	Fragment	Reaction
122	$C_6H_5SiH_2CH_3^+$	I	136	$C_6H_5SiH(CH_3)_2^+$	I	150	$C_6H_5Si(CH_3)_3^+$	I
121	$C_6H_5SiHCH_3^+$	P	135	$C_6H_5Si(CH_3)_2^+$	P	135	$C_6H_5Si(CH_3)_2^+$	P
120	$C_6H_5SiCH_3^+$	C	121	$C_6H_5SiHCH_3^+$	P	107	$C_6H_7Si^+$	C
107	$C_6H_5SiH_2^+$	P	106	$C_6H_5SiH^+$	C	105	$C_6H_5Si^+$	C
105	$C_6H_5Si^+$	C	105	$C_6H_5Si^+$	C	77	$C_6H_5^+$	P
78	$C_6H_6^+$	C	79	$C_6H_7^+$	N	74	$C_3H_{10}Si^+$	N
77	$C_6H_5^+$	P	78	$C_6H_6^+$	C	73	$(CH_3)_3Si^+$	P
69	$C_3H_5Si^+$	N	77	$C_6H_5^+$	P	67.5	$C_6H_5Si(CH_3)_2^{++}$	DP
59	$C_2H_7Si^+$	N	68	$C_6H_5SiH(CH_3)_2^{++}$	DI	53	C_2HSi^+	N
45	CH_5Si^+	P	67.5	$C_6H_5Si(CH_3)_2^{++}$	DP	43	CH_3Si^+	C
44	CH_4Si^+	C	60.5	$C_6H_5SiHCH_3^{++}$	DP			
43	CH_3Si^+	C	59	$(CH_3)_2SiH^+$	P			
28	$C_2H_4^+, N_2,$ $C_2H_4^+$	N	58	$(CH_3)_2Si^+$	C			
			43	CH_3Si^+	C			

The Table 4 shows also information about origin of the fragments. The fragments from mass spectra, which appeared during ionization (I) can be detected unambiguously. Then, there can be predicted, which fragments can appear during the primary bond cleavage (P). Then there are compounds, which appear during consecutive reactions (C). We did not detect the origin of some fragments (N), but they show small peak in mass spectra. As mentioned above, the consecutive reactions are described more in detail.

4.2.2 Cross sections

The second type of electron impact experiments is the determination of the relative cross section of ionic fragments resulting from the fragmentation process. The primary results of experiment were the functions of signal intensity depending on initial energy (Figure 9). Initial energy is considered as energy of electron before impact. The data were fitted according to the Wannier law (equation 9). The results of fitting are the ionization threshold values. We measured them for selected ionic fragments of MPS and TMPS compounds. The ionization threshold for DMPS was taken from literature (Table 5).

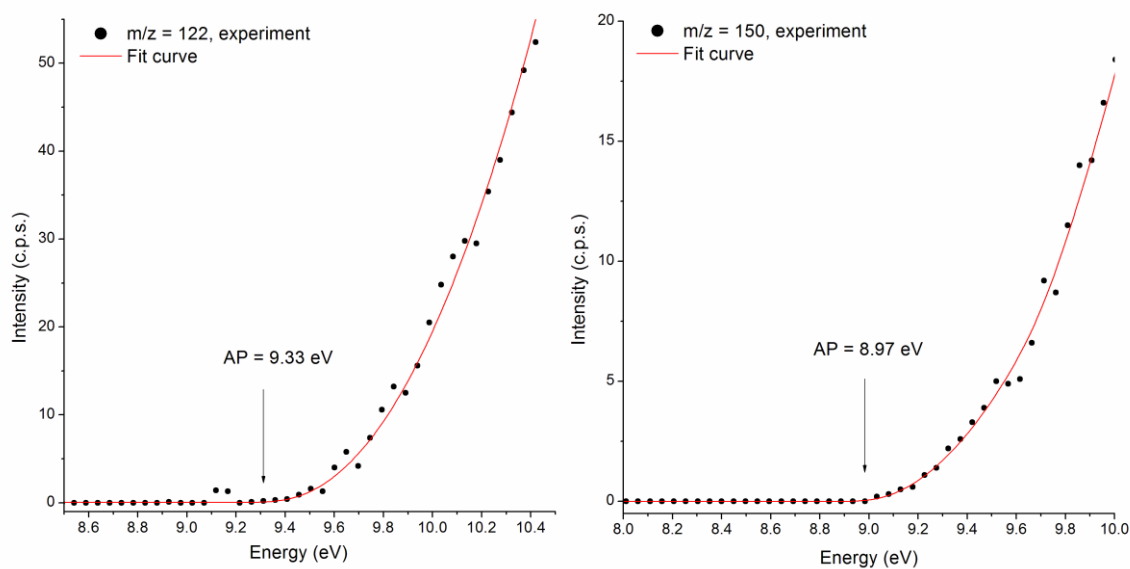


Figure 9. Ion efficiency curves near the threshold region for the parent ions of methylphenylsilane (MPS, $m/z = 122$ Th, left) and trimethylphenylsilane (TMPS, $m/z = 150$ Th, right). The measured data are shown as dark circles; the fit curves are shown as solid lines. Arrows indicate the ionization energies derived by the fitting procedure described in text.

4.2.3 Density functional theory (DFT) calculations

The computations were performed with MOLPRO program package [91]. The DFT calculations were performed to support experimental study. The Z-matrices of MPS, DMPS, and TMPS compounds and their fragments were edited by MOLDEN package [105]. Structures were optimized using the DFT calculations at the B3LYP level of theory using different basis sets. In our main calculations, we present only the results with optimal 6-311++G(d,p) basis set. The optimized geometrical structures were calculated and their energies were taken into account to compute ionization energies as well as bond dissociation energies. Appearance energies for cationic fragments were calculated from ionization energies and bond dissociation energies.

4.3 Fragmentation mechanism of organosilicones

We describe some details of the fragmentation mechanism, which consists of ionization, primary cleavage of bond, and consecutive cleavage of bonds followed by subtraction of primary fragmentation products. All the steps were described both experimentally, and by the DFT calculations. We will focus to the consecutive reactions, so the ionization and primary cleavage will be described more briefly.

4.3.1 Ionization

The ionization is the first phase of fragmentation. It can be assumed, that the reactivity of compounds is influenced by stability of cations which appear during fragmentation. The

ionization energies for MPS and TMPS neutrals were experimentally measured using previously described fitting procedure from the near threshold part of relative cross sections. The ionization energies of MPS, DMPS, and TMPS compounds were also calculated as the energy difference between the neutral molecule and its cation. The individual energies were calculated from the DFT simulation using B3LYP/6-311++G(d,p) method (Table 5).

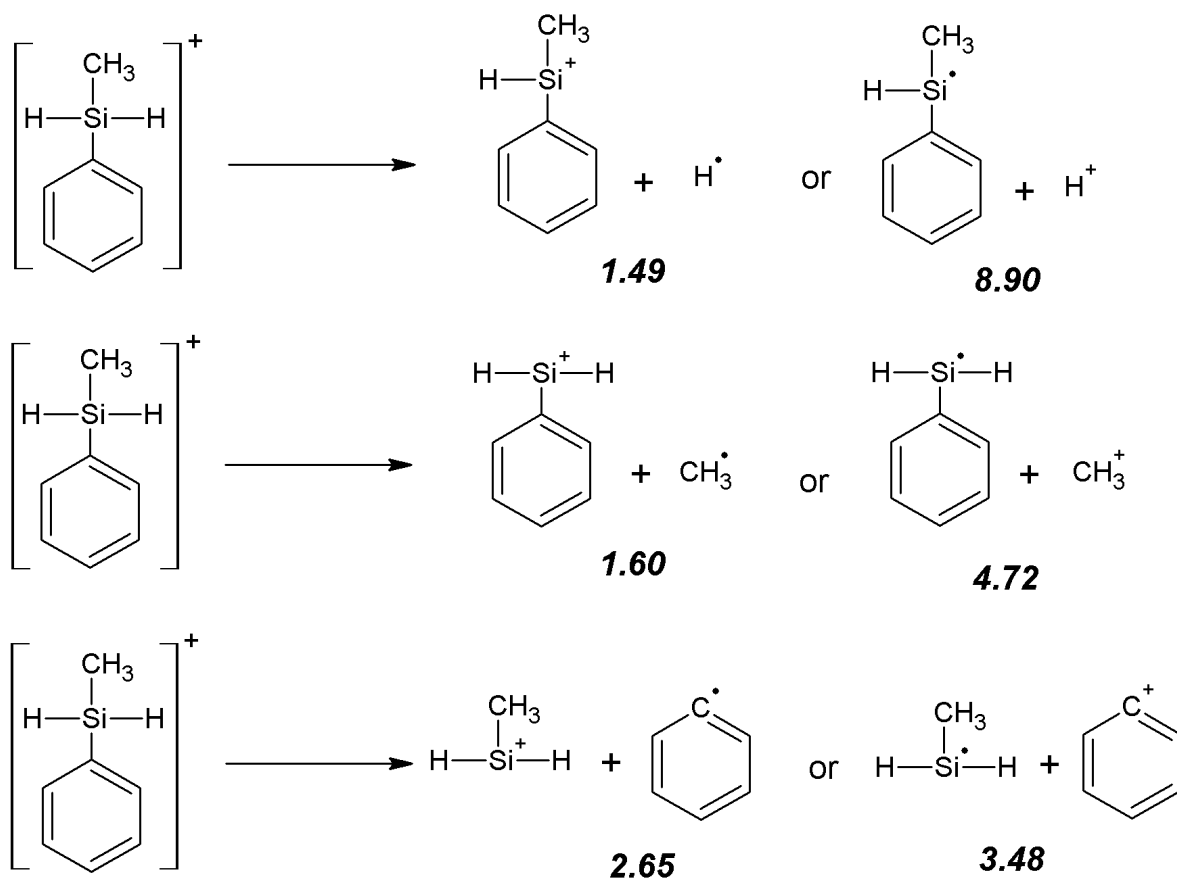
Table 5. The ionization energies for MPS, DMPS, and TMPS determined from experiment compared with the theoretical values from B3LYP/6-311++G(d,p) level.

Compound	Ionization energy (eV)	
	Experiment	Theory
MPS	9.33 ± 0.25	8.72
DMPS	9.04 ± 0.06 [17]	8.59
	8.92 ± 0.15 [18]	
	8.72 ± 0.20 [19]	
TMPS	8.97 ± 0.25	8.49
	8.81 ± 0.15 [18]	
	9.05 ± 0.03 [22]	

Both the experimental and theoretical data are more or less corresponding each to other. The theoretical values are always slightly lower than the experimental ones. Also the trends are the same. The ionization energies have relations MPS>DMPS>TMPS.

4.3.2 Primary bond cleavage

We have found that the differences between ionization energies are insignificant. There is no reason for different fragmentation products due to the ionization, so the differences should be in primary bond cleavage, where the MPS^{+•}, DMPS^{+•} and TMPS^{+•} parent metastable ionization products dissociate into more stable fragment ions. The products of such steps can be investigated systematically as there are only few bonds, which can be broken: Si-H, Si-CH₃, Si-Ph bonds and a less pronounced cleavage of different C-H bonds for these molecules. Each molecule has dissociation in order to produce one cation and one radical. The bond Si-X can be distributed both Si⁺ and X^{*} or vice versa. Thus each primary bond cleavage can produce 4 or 6 possible fragmentation products with positive charge, which can be detected in mass spectra. We do not consider any dissociation of hydrogen from CH₃ group or dissociation within the benzene ring. The comparison of the mass spectra indicates that there are some differences although such three compounds are relatively similar. For example, the position of the major peaks were recorded at $m/z = 43, 58, \text{ and } 135$, for MPS, DMPS and TMPS respectively. We can sketch the basic outline of differences between the compounds. Primary fragmentation reaction of MPS and DMPS starts with dissociation of phenyl group and on the other hand, the TMPS starts with dissociation of CH₃ group. The MPS molecule is presented as an example (Scheme 2). The reactions from Scheme 2 are associated with a single bond cleavage of H atom, CH₃ group and C₆H₅ phenyl group. There are two possibilities of fragmentation according to the distribution of the positive charge.



Scheme 2. Scheme of the H, CH₃ and C₆H₅ losses from MPS^{+•} molecular ion. The italic numbers are the bond dissociation energies (in eV) calculated using B3LYP/6-311++G(d,p) method.

The numbers in Scheme 2 are bond dissociation energies. For their evaluation, we need appearance energies (AE) of corresponding ions, which were calculated as the difference between the sum of energies of products containing the fragment ion and the energy of MPS neutral, and experimentally obtained from the fitting procedure (equation 9). We present the appearance energies from calculations and experiment in Tables 6, 7 and 8 for MPS, DMPS and TMPS, respectively.

The calculation of bond dissociation energies for theoretical and experimental data is evaluated from a difference between the appearance energy of the ionic fragment and the present value of the ionization energy (IE), or of appearance energies between two corresponding ionic fragments (equation 12).

$$BDE = AE - IE \quad (11)$$

$$BDE = AE1 - AE2 \quad (12)$$

This method (equation 11) is widely used for calculating dissociation energy of ions [18]. The bond dissociation energies and appearance energies of selected particular ions for MPS determined from experiment and calculated with theory from B3LYP/6-311++G(d,p) level are summarized in Table 6. We also compare our data which were previously calculated by Choe [19].

Table 6. The appearance energies and bond dissociation energies of selected positive ions for methylphenylsilane determined from experiment and calculated with theory from B3LYP/6-311++G(d,p) level.

m/z	Expected ion	Appearance energy (eV)		Bond dissociation energy (eV)			
		Experiment	Theory	Bond	Experiment	Theory	Theory [23]
122	MPS ⁺	9.33 ± 0.25	8.72		0	0	
121	(MPS-H) ⁺	10.56 ± 0.25	10.21	(C ₆ H ₅)(CH ₃)HSi ⁺ - H	1.23	1.49	1.37
120	(MPS-2H) ⁺	10.65 ± 0.25	14.27	(C ₆ H ₅)CH ₃ Si ⁺ - H	0.09	4.06	
120	(MPS-H ₂) ⁺		9.50			-0.71	
107	(MPS-CH ₃) ⁺	11.34 ± 0.25	10.32	(C ₆ H ₅)H ₂ Si ⁺ - CH ₃	2.01	1.60	2.01
106	(MPS-CH ₃ -H) ⁺		14.41	(C ₆ H ₅)HSi ⁺ - H		4.09	
105	C ₆ H ₅ Si ⁺	12.27 ± 0.50	16.63	C ₆ H ₅ Si ⁺ - CH ₃	1.62	2.22	
	(MPS-CH ₃ -2H) ⁺						
105	C ₆ H ₅ Si ⁺		11.86			2.36	
	(MPS-CH ₃ -H ₂) ⁺						
78	C ₆ H ₆ ⁺	9.46 ± 0.25	11.13				
77	C ₆ H ₅ ⁺		12.20	C ₆ H ₅ ⁺ - Si(CH ₃)H ₂		3.48	
69	C ₃ H ₅ Si ⁺	18 ± 0.50	13.33				
59	C ₂ H ₇ Si ⁺	11.31 ± 0.50	12.50				
45	(MPS-C ₆ H ₅) ⁺	11.76 ± 0.50	11.37	(CH ₃)H ₂ Si ⁺ - C ₆ H ₅	2.43	2.65	
44	(MPS-C ₆ H ₆) ⁺	11.28 ± 0.25	10.29	(CH ₃)HSi ⁺ - H	0.72		
43	CH ₃ Si ⁺	11.7 ± 0.50	12.44	CH ₃ Si ⁺ - H	1.05	2.23	
	(-C ₆ H ₆ -H)						
43	CH ₃ Si ⁺		12.79			3.29	
	(-C ₆ H ₅ -H ₂)						
28	Si ⁺ , N ₂ , C ₂ H ₄ ⁺	15.53 ± 0.50	16.37	Si ⁺ - C ₆ H ₅	3.26		

The single bond cleavage of the H atom, CH₃ methyl group, and C₆H₅ phenyl group leads to form ions with $m/z = 121, 107, 45$, respectively. According to the bond dissociation energies (Scheme 2), the loss of H, corresponding to the production of the $m/z = 121$ ion, is energetically more favorable than the production of the $m/z = 107$ and 45 ions. The experimental and theoretical results for the DMPS and TMPS compounds are reported in the Tables 7 and 8, respectively. The TMPS compound is different from DMPS and MPS compounds in the aspect that it does not contain the Si-H bond, where (TMPS-H)⁺ ion was not detected in mass spectrum.

Table 7. The appearance energies and bond dissociation energies of selected positive ions for dimethylphenylsilane determined from experiment and calculated with theory from B3LYP/6-311++G(d,p) level.

m/z	Expected ion	Appearance energy (eV)		Bond dissociation energy (eV)			
		Experiment [17]	Theory	Bond	Experiment [17]	Theory	Theory [23]
136	DMPS ⁺	9.04 ± 0.06	8.59		0	0	
135	(DMPS-H) ⁺	10.42 ± 0.09	9.89	(C ₆ H ₅)(CH ₃) ₂ Si ⁺ – H	1.38	1.30	1.17
121	(DMPS-CH ₃) ⁺	10.51 ± 0.15	9.92	(C ₆ H ₅)(CH ₃)HSi ⁺ – CH ₃	1.47	1.33	1.16
106	C ₆ H ₅ SiH ⁺ (-2CH ₃)	9.6 ± 0.20		(C ₆ H ₅)HSi ⁺ – CH ₃	1.34 [19] -0.91		
106	C ₆ H ₅ SiH ⁺ (-C ₂ H ₆)		10.01			0.09	
105	C ₆ H ₅ Si ⁺ (-2CH ₃ -H)	13.47 ± 0.10		C ₆ H ₅ Si ⁺ – H	3.87		
105	C ₆ H ₅ Si ⁺ (-C ₂ H ₆ -H)		12.23			2.22	
78	C ₆ H ₆ ⁺	10.2 ± 0.30	11.11				
68	DMPS ⁺²	26.3 ± 1.00	20.16				
67.5	(DMPS-H) ⁺²	27.3 ± 1.00	22.95	(C ₆ H ₅)(CH ₃) ₂ Si ⁺² – H	1.00	2.79	
60.5	(DMPS-CH ₃) ⁺²	29.3 ± 1.00	23.26	(C ₆ H ₅)(CH ₃)HSi ⁺² – CH ₃	2.00	3.10	
59	(DMPS-C ₆ H ₅) ⁺	12.4 ± 1.00	10.8	(CH ₃) ₂ HSi ⁺ – C ₆ H ₅	3.36	2.21	
58	(DMPS-C ₆ H ₆) ⁺	10.26 ± 0.14	9.69	(CH ₃) ₂ Si ⁺ – H	-0.16	-0.20	
43	CH ₃ Si ⁺	13.9 ± 0.20	12.16	CH ₃ Si ⁺ – CH ₃	3.64	2.47	

Table 8. The appearance energies and bond dissociation energies of selected positive ions for trimethylphenylsilane determined from experiment and calculated with theory from B3LYP/6-311++G(d,p) level. For fragment with $m/z = 105$ we report the average bond energy* of PhSi⁺-CH₃ bond.

m/z	Expected ion	Appearance energy (eV)		Bond dissociation energy (eV)		
		Experiment	Theory	Bond	Experiment	Theory
150	TMPS ⁺	8.97 ± 0.25	8.49		0	0
135	(TMPS-CH ₃) ⁺	9.76 ± 0.25	9.57	(C ₆ H ₅)(CH ₃) ₂ Si ⁺ – CH ₃	0.79	1.08
107	C ₆ H ₇ Si ⁺	14.54 ± 0.25	15.88			
105	(TMPS-3CH ₃) ⁺	16.93 ± 0.50	16.02	*C ₆ H ₅ Si ⁺ – CH ₃	2.65*	2.51*
77	C ₆ H ₅ ⁺	12.5 ± 0.50	12.25	C ₆ H ₅ ⁺ – Si(CH ₃) ₃	3.53	3.76
74	C ₃ H ₁₀ Si ⁺	10.69 ± 0.50	13.63			
73	(TMPS-C ₆ H ₅) ⁺	11.29 ± 0.50	10.32	(CH ₃) ₂ Si ⁺ – C ₆ H ₅	2.32	1.83
67.5	(TMPS-CH ₃) ⁺²	23.79 ± 0.50	22.63			
53	C ₆ H ₅ SiH ⁺²	20.09 ± 1.00	24.07			
43	CH ₃ Si ⁺	11.5 ± 0.50	12.41			

As mentioned above, the Tables 6-8 are important for calculation of energy profile of reactions. They can be used in general for any fragmentation reaction including the consecutive reactions discussed later. The energy profile of any reaction is a difference of B3LYP energies on the left and right side of equation. In the next text, the conclusions from theoretically calculated data for supporting of the mechanisms are presented. However, the experimental data qualitatively follow the theoretical ones. One can calculate the bond dissociation energies from experimental data.

The description of asymmetric bond cleavage can be one indication, that the results from models can be used for interpretation of real mass spectra. The primary cleavage of some selected bond can have two variants. For example, the bond cleavage presented in the Scheme 2 leads to the production of CH_3^+ cation with $m/z = 15$ and complementary radical. The second variant is the production of ion $(\text{MPS-CH}_3)^+$ with $m/z = 107$ and CH_3 radical. Only the ions are detectable in mass spectra.

We compare the energies from Scheme 2 and the $m/z = 107$ ion, is energetically more preferred than the production of CH_3 cation. This result has correlation with mass spectrum, where the intensity of the ion with $m/z = 107$ is higher than the ion with opposite distribution of charge. Next example is the bond cleavage of Si-Ph bond. The loss of C_6H_5 group, corresponding to the production of the $m/z = 45$ ion, is energetically more favorable than the production of C_6H_5 positive ion due to its low bond dissociation energy.

TMPS has lower value of CH_3 dissociation energy in comparison to MPS and DMPS (Table 6). This result is reflected in mass spectra of all components, where the loss of CH_3 methyl group from $\text{TMPS}^{\bullet+}$ molecular ion becomes more pronounced than the other two $\text{MPS}^{\bullet+}$ and $\text{DMPS}^{\bullet+}$ molecular ions.

In the case of MPS, the dissociation of H and CH_3 will be preferred and the $(\text{MPS-H})^+$ and $(\text{MPS-CH}_3)^+$ can be found in the mass spectrum. Also the dissociation of phenyl group leading to $(\text{MPS-C}_6\text{H}_5)^+$ can be identified in the mass spectra and the bond dissociation energies derived from experimental value of appearance energies (Tables 6 and 8) are in reasonable agreement with our theoretical prediction.

In the case of simple mechanism of single bond cleavage, there are expectable fragmentation products, which can be highlighted in mass spectra according to their value m/z (Tables 6-8). If the single bond cleavage mechanism is valid, its products should be detected in mass spectra in significantly higher intensities than the other fragments. It is not the case of any of the presented compounds. The complete mechanism must be even more complex. The mass spectra in reality contain significantly more fragmentation products, than would be expected from reactions from this and previous section. The second reason is the intensity of the peaks from primary products. The intensity of phenyl ($m/z = 77$) as an example of product of primary bond cleavage is relatively low. In contrast, the intensity of benzene peak ($m/z = 78$), which appears by consecutive reaction, is higher. The next example is a complementary molecule after decomposition of phenyl group. It has $m/z = 45$, but in mass spectra, there is major intensity peak is at $m/z = 43$. The fragments must be subject to additional consequent reactions.

4.3.3 Consequent fragmentation-subtraction of hydrogen

We would like to propose some reactions, which are generally observed in all the fragmentation mechanisms of MPS, DMPS, and TMPS. As they are applied to different original molecules, they lead to different products of fragmentation. Individual steps of mechanisms will be also analyzed by a model. The models enable us to describe the energy of individual steps in mechanism, which cannot be measured experimentally. However, the parameters needed to be calculated in order to have detailed picture of mechanism. In the second step, we demonstrate an ability of theoretical models to predict another mechanism, where the experimental work was still not performed. In our case, the new anionic mechanism is small modification of previously calculated one (electron impact), which we analyzed theoretically and experimentally. The prediction of fragmentation products can be useful during the designing the processes as it can replace significant part of experimental work. In this section, we would like to present a mechanism and its relation to the mass spectra and some general mechanism, which can be found in three compounds fragmentation. The results of the prediction are qualitative comparison, which peaks will be present in mass spectra and which peaks will have higher intensity. The quantitative comparison, which would enable us also compare the peak heights, needs the optimization of the model. We have focused on the consecutive reactions that follow the primary bond cleavage.

4.3.3.1 Cationic fragmentation mechanism

The next steps of the fragmentation process are various consecutive reactions, where these fragmentation reactions follow the primary bond cleavage. Here, we consider the fragmentation mechanism resulting from the electron detachment process from MPS compound leading to the formation of positively charged fragments or cations.

Mass spectra indicate a mixture of many products. Most frequently, the further cleavage of the Si-H, Si-CH₃ and Si-C₆H₅ bonds can be observed after a primary cleavage process. Frequent aspect observed in mass spectra is a loss of H₂. It is observed several times in the spectra MPS and DMPS. We compare two cases with different behavior. For example, the dissociation of the second H from (MPS-H)⁺ after the first H cleavage gives the ion with $m/z = 121$, which finally produces the $m/z = 120$ peak. Next example is the dissociation of CH₃ group from MPS⁺ followed by the loss of two hydrogens. This dissociation leads to produce the $m/z = 107$ before cleavage of 2H and $m/z = 105$ after.

We would like to focus to these two data sets from mass spectra of MPS: ($m/z = 122, 121, 120$ and $107, 106$ and 105). However, they have also different aspects. In the first case, the product after loss of one hydrogen atom ($m/z = 121$) is detected in relatively high intensity and then the second dissociation ($m/z = 120$) shows lower intensity. It corresponds to classic expectable mechanism. If we consider one hydrogen atom is dissociated in certain time, the dissociation of the next hydrogen needs extra time. If the reaction ends in finite time, it is sufficient for decomposition of one hydrogen atom, only. Some of the molecules dissociated two hydrogen atoms in such time, but it was minority of them. That is why intensity of peak 121 is

higher than the peak 120. The peak 122 of MPS^+ is lower than 121, as the MPS^+ is subject to other competitive reactions in the same time, not only to dissociation of hydrogen.

In the second case, the product of cleavage of one Si-H bond with $m/z = 106$ is almost absent, and there is present directly the product $(\text{MPS-CH}_3\text{-2H})^+$ (or $(\text{C}_6\text{H}_5\text{Si})^+$) with $m/z = 105$. The classic mechanism from previous paragraph can be applicable only in the special case. In general it must be valid, that energy barrier of the second decomposition of hydrogen must be minimal in comparison of the energy of the first one. We would like to demonstrate some principles, which we believe are generally valid also in other cases.

In both cases we propose energy profile of the reaction. As we mentioned above, all data which we use in Figures 21 and 22 are from theoretical calculations. The numbers at lines in the figures are the energy barrier for certain reaction in electronvolts. One can calculate some values from experimental data as a difference between the experimental appearance energies from Table 6 for certain products.

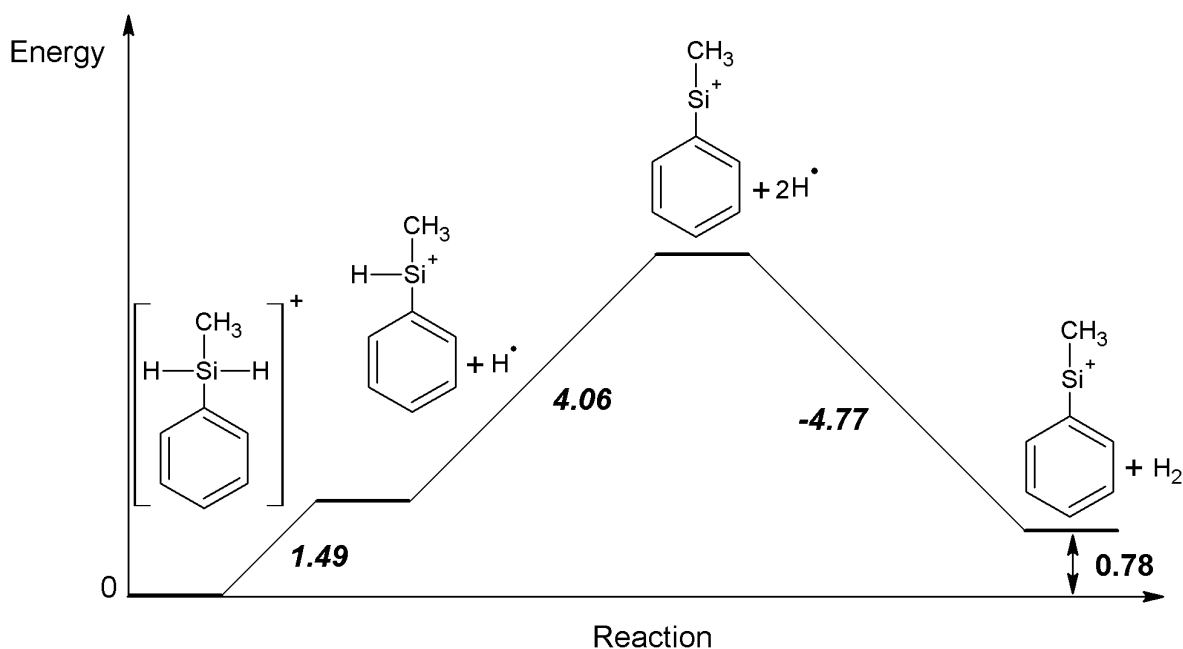


Figure 10. Energy profile for the H loss from methylphenylsilane cation derived from the B3LYP/6-311++G(d,p) calculations. The italic numbers are the bond dissociation energies (in eV).

It can be seen from Figure 10, that there is a relatively low energy barrier to decomposition of the first hydrogen, and relatively high energy barrier for decomposition of the second hydrogen. That would support the data from mass spectra, however only the relative intensities of the peaks at $m/z = 121$ and 120. The experimental bond dissociation energies are not in agreement and the dissociation of second H is only a 50 meV above the dissociation of the first H in MPS^+ (which is however below our electron energy beam resolution). The probable explanation can be found as a competitive process for C_6H_6^+ with low threshold at 9.46 eV can

be more dominant than is the loss of 2H atoms. We included also the next step – recombination of two hydrogen radicals to the hydrogen molecule, which gives to the reaction some benefit of energy. However, in the case of such mechanism the step will probably not have influence. If some recombination of radical occurs, it returns the energy usually in form of heat. This heat cannot be used directly to the dissociation of bond. All the costs of dissociation of H₂ are seemingly 0.78 eV, but in reality the energy, which was consumed (1.49+4.06) eV was consumed directly in the molecule. On the other hand, the energy of recombination (-4.77 eV) was released far from the main molecule. There is no reason, why the second dissociation of hydrogen should be favorable due to next H₂ recombination. There is only low probability, how the recombination can play a role. It is the transfer of radical after collision of H* with the segment of main molecule. However, such reaction would require exact collision of H* with some other hydrogen bonded on Si. The collision with any other atoms must be eliminated.

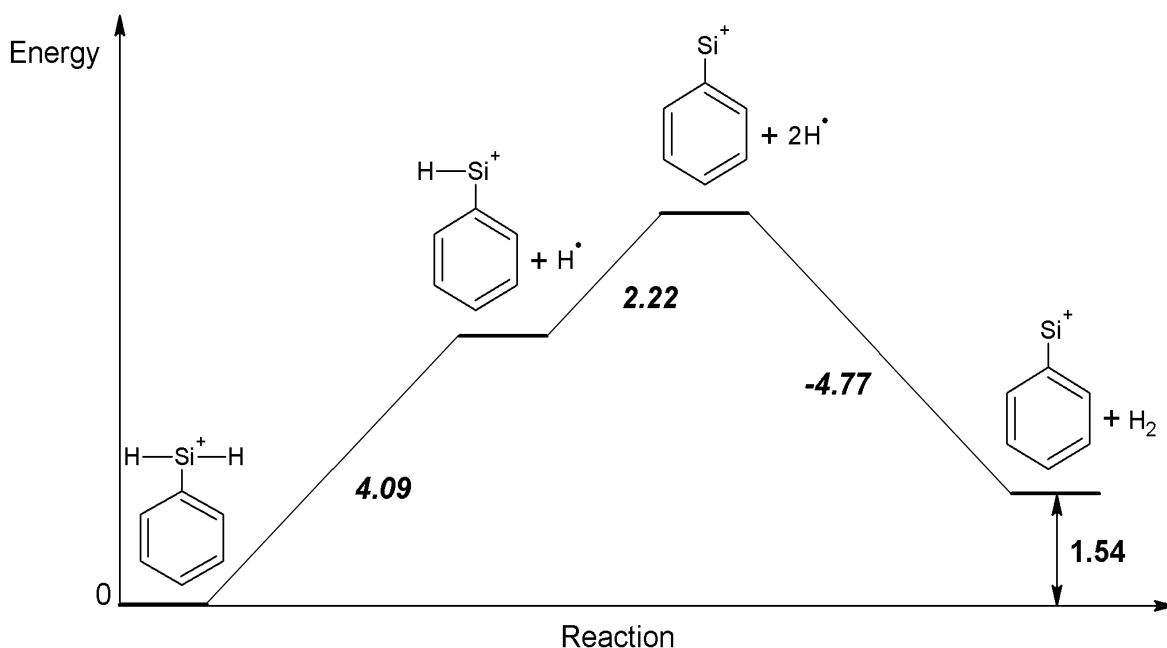


Figure 11. Energy profile for the CH₃ loss from methylphenylsilane cation derived from the B3LYP/6-311++G(d,p) calculations. The italic numbers are the bond dissociation energies (in eV).

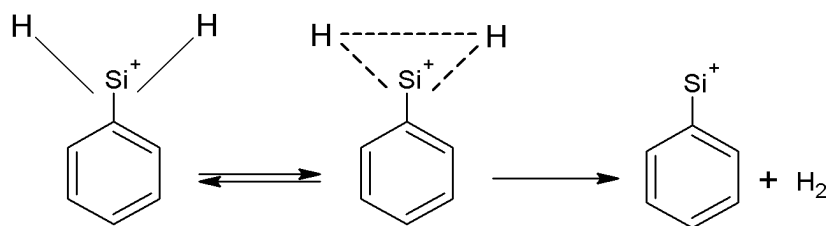
The Figure 11 shows consecutive dissociation of two hydrogen atoms from (MPS-CH₃)⁺, that is the case of peaks 107, 106 and 105. They have relatively specific picture in mass spectrum: intensive peaks 107 and 105 and small peak 106. In that case, the segment after dissociation of the first hydrogen (MPS-CH₃-H)⁺ is immediately transformed to the (MPS-CH₃-2H)⁺. The recombination of hydrogen does not play a role as well as in the previous case. In reality, we observe energy barrier of the second dissociation significantly lower than the first one. However, the energy barrier of 4.09 eV is relatively high as well as 4.06 eV from Figure 10. We can not support these results with experimental data as we were not able to measure the threshold

of the very weak $(\text{MPS-CH}_3\text{-H})^+$ ion at $m/z = 106$, however the dissociation of both hydrogens from $(\text{MPS-CH}_3)^+$ is experimentally evaluated only at 0.9 eV that is in contrast with the theoretical 6.31 eV barrier.

4.3.3.2 *New approach to the fragmentation*

We would like to propose alternative fragmentation mechanism for interpretation of mass spectra of MPS. We had hypothesis that the decomposition of hydrogen molecule could run in one step. In contrast to the classic mechanism, the energy of H_2 recombination is not lost in the heat. All energies would be consumed and released in the main molecule. The mechanism avoids a step of the decomposition of one hydrogen atom. It could explain, why in the case of $m/z = 107$ and 105 fragment with $m/z = 106$ is missing.

The mechanism consists of scissoring of the bonds (H-Si-H). In one moment, two hydrogen atoms become very close and some complex can be formed. From that complex state, they can return to initial state or continue by subtraction of hydrogen molecule. The alternative fragmentation mechanism is presented in the Scheme 3.



Scheme 3. Schematic form of the alternative fragmentation mechanism for MPS.

In reality, the reaction has still one limitation. It is because the scissoring of bonds also consumes some amount of energy. We optimized the geometry of molecule and then we compressed the shear angle. When the bond between hydrogens was undoubtedly created, the hydrogen molecule was pulled out from the fragment. The energy of such shear deformation is presented in Figure 12a. The maximum is approximately 4.25 eV. However, such value is a maximum limit value. The energy could be probably significantly lower. We reached the limit value, as we did first only bending of angle and then pulling out the hydrogen molecule from the main molecule. In reality both the partial steps run at the same time, which has a consequence in decrease of such energy barrier. We found that it could be 3.5 eV. Optimization of all the parameters procedure (bending angle, stretching, and mutual position of two hydrogens) could lead to even lower barrier.

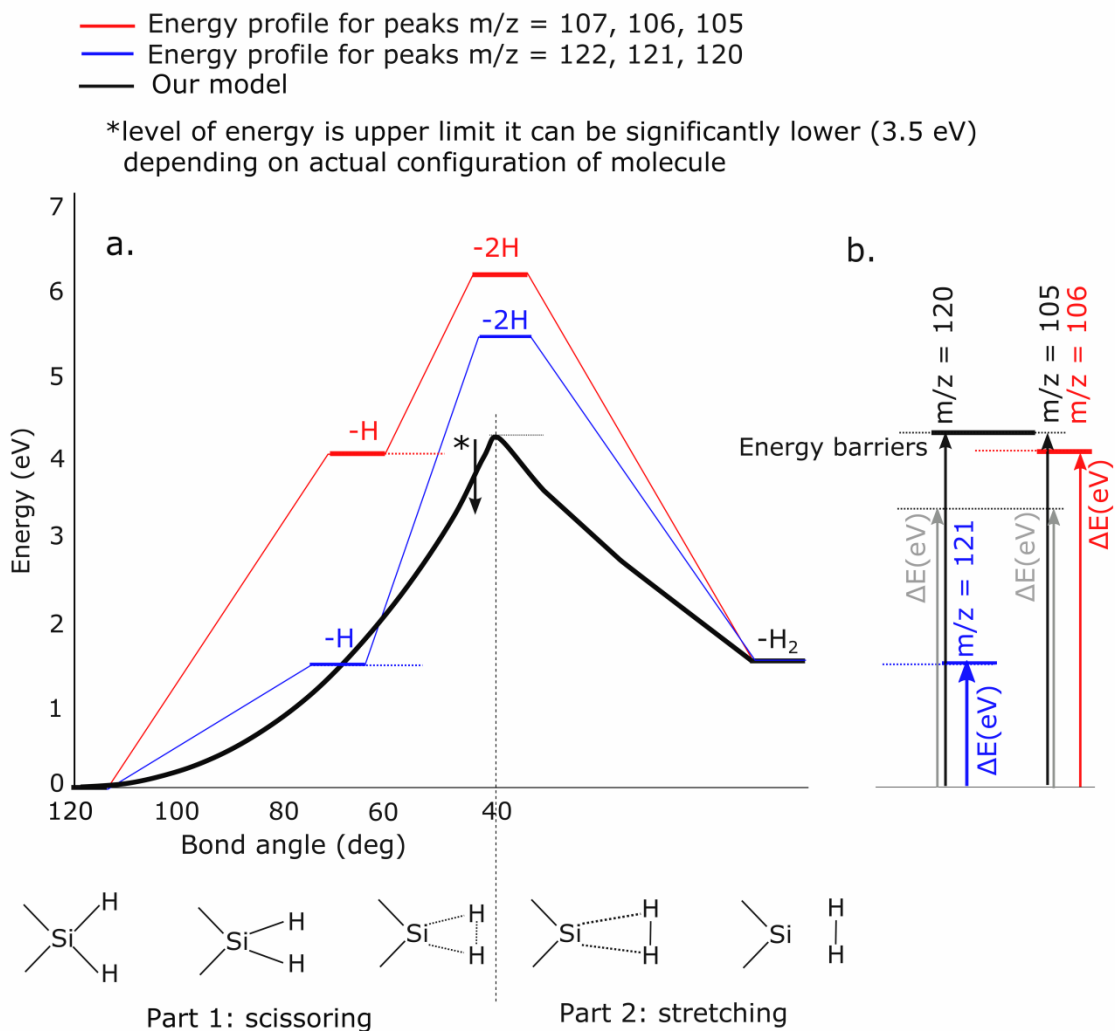


Figure 12. Energy scan for the dissociation of methylphenylsilane ion derived from the B3LYP/6-311++G(d,p) calculations.

In the case from Figure 11, the energy barrier for dissociation of two hydrogens is $4.09+2.22$, i.e. 6.31 eV. In our mechanism the barrier is approximately 3.5 eV. It might be suspected that the shear deformation of bonds could be energetically preferred. The Figure 12b shows the comparison of energy barriers for dissociation of H (blue and red arrow) or H₂ by our mechanism (grey arrow). In the first case, the blue energy barrier is related to the appearance of (MPS-H)⁺ ($m/z = 121$) and the grey energy barrier (MPS-H₂)⁺ ($m/z = 120$). The blue barrier is lower than grey. On the other hand, the red barrier creation of (MPS-CH₃-H)⁺ is higher ($m/z = 106$) than energy barrier of (MPS-CH₃-H₂)⁺ ($m/z = 105$). The comparison shows us that dissociation of H is much more probable for the peak series 122, 121 than in 107, 106. Qualitatively, it is in correlation with mass spectra, where peak 121 is relatively intensive and the peak 106 is very small.

One aspect of the optimization is the development of energy density. The Figure 13 shows the scans of electron densities from Figure 12. The Figure 13a shows the original molecule. One can see that the maximum electron density is set between Si and H atoms. So the covalent bonds Si-H exist. The Figure 13b shows the transitive state, where the Si-H bonds still partially exist, but the new one is created. Then (Figure 13c), the hydrogen molecule leaves the molecule and electron density is between the two hydrogens, this indicates that there is a new covalent bond between the hydrogens (i.e. hydrogen molecule was formed). Among these three pictures, the case b has the highest energy. It is a transitive state, where the structure can return back to the original structure or continue to dissociation of hydrogen.

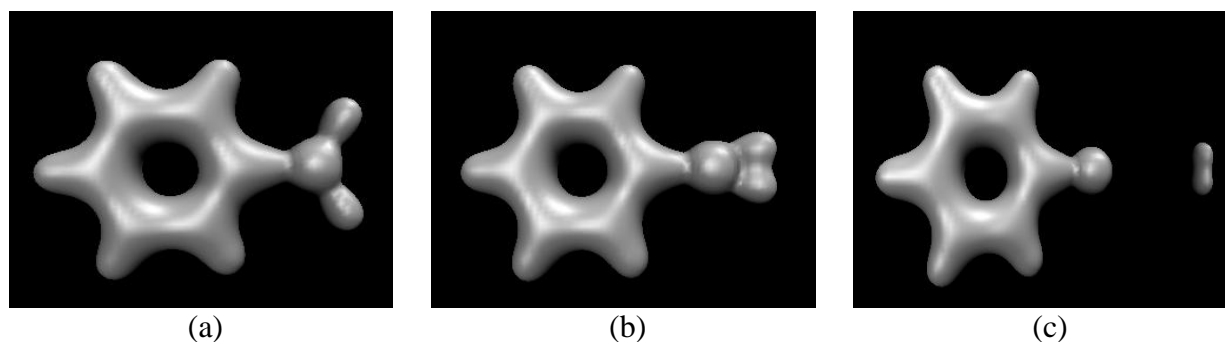


Figure 13. Electron densities plots of the $C_6H_5SiH_2^+$ fragment calculated by B3LYP/6-311++G(d,p) method.

Such mechanism can be also expected in the $m/z = 45 - 43$. The product of primary cleavage has $m/z = 45$ (dissociation of phenyl group). The next product of decomposition ($m/z = 44$) has low signal whereas the most intensive signal is $m/z = 43$. The products of the mechanism can be found in the mass spectra. It is relatively frequent pattern – double peak where the values of m/z (peak 1)- m/z (Peak 2) ≈ 2 . Such structures (ions with peaks 107/105) are visible in all the diagrams. As well peaks 95/93/91 are in all three spectra and 121/119 in TMPS.

The DMPS molecule differs from MPS, that it has only one Si-H bond. So the mechanism is not possible in form of Scheme 3 (i.e. dissociation of H_2 molecule). However, some peaks $m/z = 55/53/51$ are observed, which reflect dissociation of H_2 . However, the same mechanism can be considered also for dissociation of cationic benzene ($C_6H_6^+$) in one step (peak $m/z = 78$) instead of phenyl group and hydrogen ($m/z = 77$). The same situation (peaks $m/z 78 > 77$) can be found as well in MPS. It is only not observed in mass spectra of TMPS. The mechanism, which we proposed, requires at least one atom of hydrogen bonded on silicon. The specific property of hydrogen is that it has only one electron. If the electron is consumed to the covalent bond H-H or H-Ph, it automatically leads to dissociation of the bond H-Si. This is not the case of the CH_3 or Phenyl groups. That factor is visible in spectra TMPS. In the case, that the mechanism would be valid also for CH_3-CH_3 bond, we should see relatively intensive peak $m/z = 120$ (TMPS- C_2H_6) in the mass spectrum of TMPS. That peak is in reality rather small.

5 Final conclusions

The fragmentation energy of various molecules was calculated by quantum chemical computations: *ab initio* methods (Hartree-Fock and post-Hartree-Fock) and the density functional theory (DFT) calculations. The fragmentation energy was tested on simple molecule (propane molecule) and consequently applied to more complex compounds (organosilicon compounds) such as methylphenylsilane, dimethylphenylsilane, and trimethylphenylsilane that have similar structure. The energy calculated by quantum chemical methods can be verified by experimental work using electron impact ionization experiment. It was found that the DFT calculations are better than *ab initio* methods to investigate fragmentation process of molecules. The organosilicon compounds were selected for this study because they play a key role for understanding and developing the plasma technologies such as plasma enhanced chemical vapor deposition (PECVD), as well as silicon atoms support binding to inorganic substrates including glass, or ceramics. The fragmentation mechanism is complex. It can be seen on the mass spectra, which give general information about fragmentation products. Therefore, we have presented a combined theoretical and experimental study on organosilicones fragmentation process. We found that the calculated data are in good correlation with experimental data for electron impact ionization. Fragmentation mechanism is composed of three phases: ionization, primary bond cleavage, and consecutive reactions of bond cleavage. We found the differences in the primary bond cleavage (first cleavage after the ionization). We observed primary dissociation of phenyl group in MPS and DMPS whereas the dissociation of methyl group was primarily observed in TMPS. The organosilicon molecules release the hydrogen during the plasma induced fragmentation. We focused to mechanism of hydrogen subtraction from methylphenylsilane during plasma induced fragmentation process. The MPS in contrast to DMPS has two hydrogen atoms bounded on central silicon atom. It enables us to subtract the hydrogen molecule from the fragments. We believe that it is possible by two mechanisms. The first, classic mechanism consists of subtraction of two hydrogen atoms step-by-step. The second mechanism is the subtraction of two hydrogen atoms in one step. The second mechanism is associated with the scissoring and compression of the (H-Si-H) shear bond angle leading to consecutive subtraction of H₂ molecule. The second mechanism is observed only in special cases, when the energy barrier for the first subtraction of hydrogen is too large. Otherwise, the classic mechanism prevails. We verified by experiment particularly the relative cross-sections of cations that there is possibility to calculate also the cross-sections by theoretical calculation. The experimental data was in correlation with calculated results. We can predict which mechanism is more probable according to the DFT calculated energy profile of reaction. The calculated predictions were in correlation with the composition of fragmentation products from mass spectra.

6 References

- [1] G. Barroso, M. Morshedi, S. Oehninger, *Hum. Reprod.* 15 (2000) 1338-1344.
- [2] L. Simon, G. Brunborg, M. Stevenson, D. Lutton, J. McManus, S. E. M. Lewis, *Hum. Reprod.* 25 (2010) 1594-1608.
- [3] V. Čech, J. Studýnka, N. Conte, V. Peřina, *Surf. Coat Technol.* 201 (2007) 5512-5517.
- [4] V. Čech, J. Studýnka, F. Janoš, V. Peřina, *Plasma Process. Polym.* 4 (2007) 776-780.
- [5] V. Brites, G. Chambaud, M. Hochlaf, J. Kočišek, J. L. C. Diaz, S. Matejčík, F. Krčma, *J. Phys. Chem. A* 113 (2009) 6531-6536.
- [6] J. Kočišek, O. Stružinský, H. Sahánková, F. Krčma, Š. Matejčík, *Plasma Process. Polym.* 9 (2012) 298-303.
- [7] T. Aarii, S. Otake, Y. Takata, S. Matsuura, *J. Mass Spectrom. Soc. Jpn.* 54 (2006) 243-249.
- [8] R. L. Whetten, C. Yerezian, *Int. J. Mod. Phys. B* 6 (1992) 3801-3814.
- [9] R. Davis, M. Frearson, *Mass Spectrometry. Analytical Chemistry by Open Learning*, John Wiley & Sons, London, 1987.
- [10] Central Connecticut State University, Department of Chemistry & Biochemistry, [http://www.chemistry.ccsu.edu/glagovich/teaching/316/ms%20\(old\)/alkane-straight.html](http://www.chemistry.ccsu.edu/glagovich/teaching/316/ms%20(old)/alkane-straight.html).
- [11] L. Sleno, D. A. Volmer, *J. Mass Spectrom.* 39 (2004) 1091-1112.
- [12] R. A. Zubarev, N. L. Kelleher, F. W. McLafferty, *J. Am. Chem. Soc.* 120 (1998) 3265-3266.
- [13] L. M. Mikesh, B. Ueberheide, A. Chi, J. J. Coon, J. E. P. Syka, J. Shabanowitz, and D. F. Hunt, *Biochim. Biophys. Acta.* 1764 (2006) 1811-1822.
- [14] S. Denifl, Š. Matejčík, J. D. Skalný, M. Stano, P. Mach, J. Urban, P. Scheier, T. D. Märk, W. Barszczewska, *Chem. Phys. Lett.* 402 (2005) 80-87.
- [15] L. A. Curtiss, K. Raghavachari, P.C Redfern, V. Rassolov, J. A. Pople, *J. Chem. Phys.* 109 (1998) 7764-7776.
- [16] A. G Baboul, L. A. Curtiss, P.C Redfern, K. Raghavachari, *J. Chem. Phys.* 110 (1999) 7650-7657.
- [17] J. A. Montgomery, M. J. Frisch, J.W. Ochterski, G.A. Petersson, *J. Chem. Phys.* 110 (1999) 2822-2827.
- [18] D. L. Lichtenberger, A. S. Copenhaver, *Bonding Energetics in Organometallic Compounds*, ACS Symposium Series, Vol. 428, 1990.
- [19] J. C. Choe, *Int. J. Mass Spectrom.* 242 (2005) 5-11.
- [20] E. E. B. Campbell, F. Rohmund, *Rep. Prog. Phys.* 63 (2000) 1061-1109.
- [21] C. Lifshitz, *Int. J. Mass. Spectrom.* 200 (2000) 423-442.
- [22] S. Matt, O. Echt, T. Rauth, B. Dünser, M. Lezius, A. Stamatovic, P. Scheier, T. D. Märk, *Z. Phys. D* 40 (1997) 389-394.
- [23] T. Wakabayashi, H. Shiromaru, S. Suzuki, K. Kikuchi, Y. Achiba, *Surf. Rev. Lett.* 3 (1996) 793-798.
- [24] T. Kimura, T. Sugai, H. Shinohara, *J. Chem. Phys.* 110 (1999) 9681-9687.

- [25] R. D. Beck, P. Weis, J. Rockenberger, R. Michel, D. Fuchs, M. Benz, M. M. Kappes, *Surf. Rev. Lett.* 3 (1996) 881-885.
- [26] J. McMurry, *Organic chemistry*, Thomson Brooks/Cole, 2008, pp. 426.
- [27] S. G. Lias, "*Mass Spectrum (electron ionization)*" in *NIST Chemistry WebBook*, *NIST Standard Reference Database Number 69*. Available from: <http://webbook.nist.gov/chemistry/>.
- [28] E. Vašeková, M. Stano, Š. Matejčík, J. D. Skalný, P. Mach, J. Urban, T. D. Märk, *Int. J. Mass Spectrom.* 235 (2004) 155-162.
- [29] J. M. Gaidis, P. R. Briggs, T. W. Shannon, *J. Phys. Chem.* 75 (1971) 974-980.
- [30] S. T. Nakagawa, I. Suzue, M. Itoh, M. Kageyama, Y. Mizuno, H. J. Whitlow, *J. Nucl. Mater.* 363-365 (2007) 1289-1293.
- [31] L. Hanley, J. L. Whitten, S. L. Anderson, *J. Phys. Chem.* 92 (1988) 5803-5812.
- [32] A. K. Ray, I. A. Howard, K. M. Kanal, *Phys. Rev. B* 45 (1992) 14247-14255.
- [33] H. Kato, K. Yamashita, K. Morokuma, *Chem. Phys. Lett.* 190 (1992) 361-366.
- [34] G. A. Dolgonos, G. H. Peslherbe, *Chem. Phys. Lett.* 398 (2004) 217-223.
- [35] W. C. Eckhoff, G. E. Scuseria, *Chem. Phys. Lett.* 216 (1993) 399-404.
- [36] A. D. Boese, G. E. Scuseria, *Chem. Phys. Lett.* 294 (1998) 233-236.
- [37] R. E. Stanton, *J. Chem. Phys.* 96 (1992) 111-118.
- [38] J. Y. Yi, J. Bernholc, *J. Chem. Phys.* 96 (1992) 8634-8636.
- [39] C. H. Xu, G. E. Scuseria, *Phys. Rev. Lett.* 72 (1994) 669-672.
- [40] B. L. Zhang, C. H. Xu, C. Z. Wang, C. T. Chan, K. M. Ho, *Phys. Rev. B* 46 (1992) 7333-7336.
- [41] S. Matt, O. Echt, P. Scheier, T. D. Märk, *Chem. Phys. Lett.* 348 (2001) 194-202.
- [42] S. Tomita, J. U. Andersen, C. Gottrup, P. Hvelplund, U. V. Pedersen, *Phys. Rev. Lett.* 8707 (2001) 073401-073404.
- [43] M. Born, R. Oppenheimer, *Ann. Phys.* 389 (1927) 457-484.
- [44] E. Schrodinger, *Phys. Rev.* 28 (1926) 1049-1070.
- [45] M. Šob, M. Friák, D. Legut, J. Fiala, V. Vitek, *Mat. Sci. Eng. A* 387-389 (2004) 148-157.
- [46] J. B. Foresman, Æ. Frisch, *Exploring Chemistry with Electronic Structure Methods*, Gaussian, Inc., U. S. A., 2000.
- [47] D. R. Hartree, *Proc. Comb. Phil. Soc.* 24 (1928) 111-132.
- [48] P. W. Atkins, R. S. Friedman, *Molecular Quantum Mechanics*, Oxford University Press, 1999.
- [49] J. B. Foresman, M. H. Gordon, J. A. Pople, M.J. Frisch. *J. Phys. Chem.* 96 (1992) 135-149.
- [50] E. G. Lewars, *Computational Chemistry: Introduction to the Theory and Applications of Molecular and Quantum Mechanics*, Kluwer Academic Publishers, 2003.
- [51] A. R. Leach, *Molecular Modelling: Principles and Applications*, Addison Wesley Longman Limited, 1996.

- [52] W. J. Hehre, L. Radom, Paul. V. R. Schleyer, John A. Pople, *Ab Initio* Molecular Orbital Theory, John Wiley & Sons, Inc., 1986.
- [53] K. Raghavachari, J. B. Anderson, *J. Phys. Chem.* 100 (1996) 12960-12973.
- [54] C. Møller, M.S. Plesset, *Phys. Rev.* 46 (1934) 618-622.
- [55] R. J. Bartlett, *Annu. Rev. Phys. Chem.* 32 (1981) 359-401.
- [56] C. D. Sherrill, H. F. Schaefer, *Adv. Quant. Chem.* 34 (1999) 143-269.
- [57] I. Shavitt, *The Method of Configuration Interaction*, in: *Methods of Electronic Structure Theory*, Plenum Press, New York, 1977.
- [58] M. Mueller, *Fundamentals of Quantum Chemistry: Molecular Spectroscopy and Modern Electronic Structure Computations*, Kluwer Academic/Plenum Publishers, New York, 2001.
- [59] F. Jensen, *Introduction to Computational Chemistry*, John Wiley & Sons, Ltd., 2007.
- [60] D. C. Young, *Computational Chemistry: A Practical Guide for Applying Techniques to Real World Problems*, John Wiley & Sons, Inc., 2001.
- [61] J. Čížek, *J. Chem. Phys.* 45 (1966) 4256-4267.
- [62] J. Čížek, J. Paldus, *Int. J. Quantum Chem.* 5 (1971) 359-379.
- [63] R. J. Bartlett, *J. Phys. Chem.* 93 (1989) 1697-1708.
- [64] J. A. Pople, R. Krishnan, HB. Schlegel, JS. Binkley, *Int. J. Quantum Chem.* 14 (1978) 545-560.
- [65] G. D. Purvis III, RJ. Bartlett, *J. Chem. Phys.* 76 (1982) 1910-1918.
- [66] J. Noga, RJ. Bartlett, *J. Chem. Phys.* 86 (1987) 7041-7050.
- [67] J. A. Pople, J. S. Binkley, R. Seeger, *Int. J. Quantum Chem. Symp.* 10 (1976) 1-19.
- [68] Z. He, D. Cremer, *Theor. Chim. Acta.* 85 (1993) 305-323.
- [69] M. W. Schmidt, M. S. Gordon, *Annu. Rev. Phys. Chem.* 49 (1998) 233-266.
- [70] L. M. Cheung, K. R. Sundberg, K. Ruedenberg, *Int. J. Quantum Chem.* 16 (1979) 1103-1137.
- [71] B. O. Roos, *Adv. Chem. Phys.* 69 (1987) 399-445.
- [72] P. Hohenberg, W. Kohn, *Phys. Rev.* 136 (1964) 864-871.
- [73] W. Kohn, L. J. Sham, *Phys. Rev.* 140 (1965) 1133-1138.
- [74] R. G. Parr, W. Yang, *Density Functional Theory of Atoms and Molecules*, International Series of Monographs on Chemistry, Oxford University Press, New York, 1989.
- [75] A. D. Becke, *J. Chem. Phys.* 98 (1993) 5648-5652.
- [76] J. P. Perdew, K. Burke, Y. Wang, *Phys. Rev. B* 54 (1996) 16533-16539.
- [77] D. Joubert, *Density Functionals: Theory and Applications*, Springer-Verlag, Heidelberg, 1998.
- [78] E. Tasal, M. Kumalar, *Spectrochim. Acta, Part A* 95 (2012) 282-299.
- [79] R. J. Xavier, S. A. Raj, *Spectrochim. Acta, Part A* 101 (2013) 148-155.
- [80] L. Padmaja, C. Ravikumar, D. Sajan, I. H. Joe, V. S. Jayakumar, G. Pettit, O. F. Nielsen, *J. Raman Spectrosc.* 40 (2009) 419-428.
- [81] C. Ravikumar, I. H. Joe, V. S. Jayakumar, *Chem. Phys. Lett.* 460 (2008) 552-558.

- [82] C. H. Lin, H. L. Chen, L. A. Wang, *Microelectron. Eng.* 57-58 (2001) 555-561.
- [83] R. Morent, N. D. Geyter, S. V. Vlierberghe, P. Dubruel, C. Leys, L. Gengembre, E. Schacht, E. Payen, *Prog. Org. Coat.* 64 (2009) 304-310.
- [84] V. Cech, A. Knob, H. Hosein, A. Babik, L. Drzal, *Proc. Int. Conf. Composite Interfaces (Interface 21)*, (2012) 1-4.
- [85] R. Barni, S. Zanini, C. Riccardi, *Adv. Phys. Chem.* 2012 (2012) 205380–205386.
- [86] K. Igawa, J. Takada, T. Shimono, K. Tomooka, *J. Am. Chem. Soc.* 130 (2008) 16132-16133.
- [87] S. E. Denmark, C. R. Butler, *J. Am. Chem. Soc.* 130 (2008) 3690-3704.
- [88] J. C. Choe, *Rapid Commun. Mass Spectrom.* 17 (2003) 207-211.
- [89] J. C. Choe, *Int. J. Mass Spectrom.* 237 (2004) 1-12.
- [90] T. Veszprémi, Y. Harada, K. Ohno, H. J. Mutoh, *J. Organomet. Chem.* 266 (1984) 9-16.
- [91] MOLPRO, version 2010.1, A package of *ab initio* programs, H. J. Werner, P. J. Knowles, G. Knizia, F. R. Manby, M. Schütz, and others. Available from: <http://www.molpro.net>.
- [92] D. Chhabil, *Fundamentals of Contemporary Mass Spectrometry*, John Wiley & Sons, 2007.
- [93] G. Dube, V. Chvalovský, *Collect. Czech. Chem. Commun.* 39 (1974) 2621-2629.
- [94] I. Kuritka, P. Broza, J. Prycek, F. Schauer, *Plasma Process. Polym.* 4 (2007) 53-61.
- [95] M. Stano, Š. Matejčík, J. D. Skalný, T. D. Märk, *J. Phys. B: At. Mol. Opt. Phys.* 36 (2003) 261-271.
- [96] S. G. Lias, "*Ion Energetic Data*" in *NIST Chemistry WebBook, NIST Standard Reference Database Number 69*. Available from: <http://webbook.nist.gov/chemistry/>.
- [97] G. H. Wannier, *Phys. Rev.* 90 (1953) 817-825.
- [98] Y. K. Kim, W. Hwang, N. M. Weinberger, M. A. Ali, M. E. Rudd, *J. Chem. Phys.* 106 (1997) 1026-1033.
- [99] K. N. Joshipura, C. G. Limbachiya, *Int. J. Mass Spectrom.* 216 (2002) 239-247.
- [100] P. McCallion, M. B. Shah, H. B. Gilbody, *J. Phys. B: At., Mol. Opt. Phys.* 25 (1992) 1061-1071.
- [101] K. Fujii, S. K. Srivastava, *J. Phys. B: At., Mol. Opt. Phys.* 28 (1995) L559-L563.
- [102] D. P. Almeida, M. A. Scopel, R. R. Silva, A. C. Fontes, *Chem. Phys. Lett.* 341 (2001) 490-494.
- [103] Y. K. Kim, M. E. Rudd, *Phys. Rev. A: At. Mol. Opt. Phys.* 50 (1994) 3954-3967.
- [104] H. Deutsch, K. Becker, S. Matt, T.D. Märk, *Int. J. Mass Spectrom.* 197 (2000) 37-69.
- [105] G. Schaftenaar, J. H. Noordik, *J. Comput. Aided Mol. Des.* 14 (2000) 123-134.
- [106] B. K. Sharma, *Spectroscopy*, Krishna Prakashan Media Meerut, 2007, ISBN: 8182830184.
- [107] C. D. Finney, A. G. Harrison, *Int. J. Mass Spectrom. Ion Phys.* 9 (1972) 221-233.
- [108] G. Bieri, F. Burger, E. Heilbronner, J. P. Maier, *Helv. Chim. Acta.* 60 (1977) 2213-2233.

7 Curriculum Vitae

Author of this thesis was born on 21st March 1982 in Aleppo-Syria. In 2010, he started his Ph.D. studies at Brno University of Technology, Faculty of Chemistry, Institute of Physical and Applied Chemistry (IPAC) focusing on modelling of chemical processes using quantum chemical computations. He contributed to conferences and journals listed below.

Conferences

- A. Al Sheikh, J. Žídek, F. Krčma, 5th Meeting on Chemistry and Life, Brno, Czech Republic, The calculation of fragmentation energy of organometallic compounds by using *ab initio* method, Chemické listy, 2011, vol. 105, pp. 893-894, ISSN: 0009-2770.
- A. Al Sheikh, J. Žídek, F. Krčma, International Conference on Plasma Physics, Venice, Italy, Description of kinetics of propane fragmentation with a support of *ab initio* simulation, An international journal of science, World Academy of Science, Engineering and Technology, 2012, vol. 71, pp. 69-72, ISSN: 2010- 376X.
- M. Lacko, A. Al Mahmoud Alsheikh, P. Papp, Š. Matejčík, In Proceedings of 6th Conference on Elementary Processes in Atomic Systems (CEPAS), Bratislava, Slovakia, The ligand dissociations from MPS, DMPS and TMPS molecules by electron impact, 2014, pp. 53-57, ISBN: 978-80-8147-021- 9.
- A. Al Mahmoud Alsheikh, J. Žídek, F. Krčma, P. Papp, M. Lacko, Š. Matejčík, In book of abstracts of CEITEC Annual Conference "Frontiers in Material and Life Sciences", Brno, Czech Republic, Mechanism of hydrogen subtraction from methylphenylsilane during plasma induced fragmentation process, 2014, pp. 81, ISBN: 978-80-210-7159-9.
- Michal Lacko, Peter Papp, Amer Al Mahmoud Alsheikh, Jan Žídek, František Krčma, Štefan Matejčík, In the book of contributed papers of 20th conference on Symposium on Application of Plasma Processes (SAPP), Bratislava, Slovakia, A complex study of electron impact ionisation and dissociation of methyl-, dimethyl- and trimethylphenylsilane, 2015, pp. 210-213, ISBN: 978-80-8147-027- 1.

Participation at projects

- Praktická úloha zaměřená na simulaci a experimentální ověření fragmentace organosilikonových molekul.
- Fyzikálně-chemické procesy a jejich aplikace.
- Studium fyzikálně chemických procesů pro budoucí aplikace.
- Výzkum fyzikálně chemických procesů s ohledem na jejich aplikační potenciál.
- Fyzikálně-chemické procesy – jejich výzkum a aplikace.

Short Stays

Comenius University, Faculty of Mathematics, Physics and Informatics, Department of Experimental Physics in Slovakia, Performance of electron impact ionization experiments. 1/3/2014-15/3/2014.

Articles

- Ibrahim E. El-Shamy, A. M. Abdel-Mohsen, Amer A. Alsheikh, Moustafa M. G. Fouda, Salem S. Al-Deyab, Maher A. El-Hashash, J. Jancar, Synthesis, biological, anti-inflammatory activities and quantum chemical calculation of some [4-(2, 4, 6-trimethylphenyl)-1(2H)-oxo-phthalazin-2yl] acetic acid hydrazide derivatives, *Dyes Pigm.* 113 (2015) 357-371.
- Ibrahim E. El-Shamy, A. M. Abdel-Mohsen, Amer A. Alsheikh, Moustafa M. G. Fouda, Salem S. Al-Deyab, Maher A. El-Hashash, Synthesis and antimicrobial activities of S-nucleosides of 4-mesitylphthalazine-1-thiol and some new selenium-containing nucleoside analogues, *Tetrahedron Lett.* XXX (2015) XXX-XXX.
- Amer Al Mahmoud Alsheikh, Jan Žídek, František Krčma, Peter Papp, Michal Lacko, Štefan Matejčík, Fragmentation of methylphenylsilane and trimethylphenylsilane: A combined theoretical and experimental study, *Int. J. Mass Spectrom.*, under review.